# UNIVERSITA' DEGLI STUDI DI VERONA

*DEPARTMENT OF*

*DIAGNOSTIC AND PUBLIC HEALTH*

*GRADUATE SCHOOL OF*

*NATURAL AND ENGINEERING SCIENCES*

*DOCTORAL PROGRAM IN*

*NANOSCIENCES AND ADVANCED TECHNOLOGIES*

Cycle / year 31°

# ADIPOSE-DERIVED MULTIPOTENT STROMAL CELLS IN REGENERATIVE MEDICINE

S.S.D. BIO/16 ANATOMIA UMANA - BIO/17 ISTOLOGIA

Coordinator: Prof. Tagliaro Franco

Signature _____

Tutor: Prof. Sbarbati Andrea

Signature _____

Doctoral Student: Dott.ssa Dai Prè Elena

Signature _____

## TABLE OF CONTENTS


1. SUMMARY ..... 6
2. ABSTRACT ..... 7
3. INTRODUCTION ..... 8
   3.1. The biology of adipose tissue ..... 8
   3.2. Adipose Stromal Vascular Fraction (SVF) ..... 10
      3.2.1. Multipotent stromal cells (MSCs) ..... 10
         3.2.1.1. Adipose-derived stromal cells (ASCs) ..... 11
         3.2.1.2. Multipotent stress-enduring stem cells (MUSE) ..... 11
4. REGENERATION AND RECONSTRUCTION THROUGH ADIPOSE TISSUE ..... 12
   4.1. Autologous fat grafting ..... 12
      4.1.1. History of fat grafting ..... 12
      4.1.2. Complications and limitations ..... 13
      4.1.3. Cell-assisted lipotransfer (CAL) ..... 14
      4.1.4. Platelet-rich plasma (PRP) ..... 14
      4.1.5. Fat grafting technique ..... 15
         4.1.5.1. Fat harvesting ..... 15
         4.1.5.2. Fat processing ..... 15
            4.1.5.2.1. Enzymatic methods ..... 16
         4.1.5.3. Fat delivery ..... 21
      4.1.6. How does the fat grafting occur? ..... 22
      4.1.7. Characterization of ASCs-rich micrografts obtained from different devices 23
         4.1.7.1. General introduction ..... 23
         4.1.7.2. Rigenera® (Human brain Wave, Turin) ..... 23
            4.1.7.2.1. Introduction ..... 23
            4.1.7.2.2. Material and methods ..... 24
            4.1.7.2.3. Results ..... 27
            4.1.7.2.4. Discussion ..... 36
            4.1.7.2.5. Conclusion ..... 37
         4.1.7.3. Hy-tissue SVF® (Fidia Farmaceutici, Abano Terme, Padua, Italy) ..... 38
            4.1.7.3.1. Introduction ..... 38

4.1.7.3.2. Material and methods ..... 39
4.1.7.3.3. Results ..... 43
4.1.7.3.4. Discussion ..... 49
4.1.7.3.5. Conclusion ..... 49
4.1.7.4. Hy-tissue Nanofat® (Fidia Farmaceutici, Abano Terme, Padua, Italy) 50
4.1.7.4.1. Introduction ..... 50
4.1.7.4.2. Material and methods ..... 51
4.1.7.4.3. Results ..... 53
4.1.7.4.4. Discussion ..... 58
4.1.7.4.5. Conclusion ..... 58
4.1.7.4. General conclusion ..... 59
4.2. Adipose tissue engineering ..... 60
4.2.1. Introduction ..... 60
4.2.1.1. What is tissue engineering? ..... 60
4.2.1.2. Hyaluronic acid ..... 61
4.2.1.3. Hyaluronic acid hydrogels for tissue engineering ..... 62
4.2.1.4. Mechanism of cell behavior regulation by hyaluronic acid ..... 63
4.2.1.5. Application of HA-based scaffold pre-seeded with MSCs in regenerative medicine ..... 63
4.2.2. *In vitro* interaction among hyaluronic acid and ASCs ..... 64
4.2.2.1. Introduction ..... 64
4.2.2.2. Material and methods ..... 64
4.2.2.2.1. Hyaluronic acid formulations ..... 64
4.2.2.2.2. Adipose tissue samples collection ..... 64
4.2.2.2.3. Cell isolation and culture ..... 65
4.2.2.2.4. Powders and fillers: citotoxicity assay ..... 65
4.2.2.2.5. Powders and fillers: adipogenesis evaluation ..... 66
4.2.2.2.6. FID-119 sponge: transmission electron microscopy (TEM) of ASCs after incubation with FID-119 ..... 66
4.2.2.2.7. FID-119 sponge: scanning electron microscopy (SEM) of ASCs after incubation with FID-119 ..... 67
4.2.2.2.8. FID-119 sponge: histological analysis ..... 68
4.2.2.3. Results ..... 69

4.2.2.3.1. Powders and fillers ..... 69
4.2.2.3.2. FID-119 sponge ..... 74
4.2.2.4. Discussion ..... 77
4.2.2.5. Conclusion ..... 77
4.2.3. *In vivo* interaction among hyaluronic acid and fat ..... 77
4.2.3.1. Introduction ..... 77
4.2.3.2. Material and methods ..... 78
4.2.3.2.1. Hyaluronic acid formulations ..... 78
4.2.3.2.2. Adipose tissue collection ..... 78
4.2.3.2.3. Animals ..... 78
4.2.3.2.4. Magnetic resonance imaging (MRI) ..... 79
4.2.3.2.5. 3D reconstruction of subcutaneous implants ..... 79
4.2.3.2.6. Histology of subcutaneous implants ..... 80
4.2.3.3. Results ..... 81
4.2.3.4. Discussion ..... 83
4.2.3.5. Conclusion ..... 83
5. CONCLUSION ..... 84
6. REFERENCES ..... 85

# *1. SUMMARY*

Nonostante il tessuto adiposo sia stato considerato per molti anni un prodotto di scarto, è stato recentemente riconosciuto il suo ruolo come agente rigenerativo. Il tessuto adiposo è un tessuto connettivo costituito da adipociti interspersi in fibre di collagene e dalla frazione vasculo-stromale (SVF), composta da cellule stromali multipotenti adipose (ASCs), pre-adipociti, fibroblasti, cellule vascolari endoteliali e cellule del sistema immunitario. Il ruolo rigenerativo è svolto principalmente dall'SVF e, in esso, specialmente dalle ASCs, secernendo fattori di crescita angiogenetici, anti-apoptotici, anti-infiammatori e immunomodulatori.

I chirurghi usano diverse strategie per ricostruire o riparare i tessuti e gli organi danneggiati attraverso il tessuto adiposo. Tra esse, le più efficienti sono il trasferimento autologo di tessuto adiposo e l'ingegneria tissutale. Nel trasferimento autologo di tessuto adiposo, il tessuto adiposo autologo è prelevato da una parte del corpo, purificato attraverso alcune tecniche di processazione e ri-iniettato dove necessario. Nell'ingegneria tissutale, alcuni scaffold fatti di materiali naturali o sintetici sono usati in combinazione con le ASCs e, talvolta, con fattori di crescita, per riparare o ricostruire tessuti.

La prima parte sperimentale di questa tesi di dottorato analizza le performance *in vitro* di un dispositivo medico automatizzato e di due diversi kit monouso per processare il tessuto adiposo a confronto con la digestione enzimatica, che è la tecnica gold-standard. Tutti tre i metodi producono microinnesti ricchi di ASCs. Parametri come il fenotipo, la vitalità, la crescita e la replicazione delle ASCs sono stati osservati.

La seconda parte sperimentale di questa tesi analizza le performance *in vitro* e *in vivo* di differenti formulazioni di acido ialuronico, un materiale naturale e molto promettente per rigenerare i tessuti, quando combinato con le ASCs. Parametri come la vitalità delle ASCs, la loro interazione con le formulazioni di acido ialuronico e l'adipogenesi sono stati osservati.

# 2. ***ABSTRACT***

Beside adipose tissue had been considered a discard product for many years, recently its role as regenerative agent has been widely recognized. Adipose tissue is a connective tissue constituted of adipocytes interspersed with collagen fibers and stromal vascular fraction (SVF), composed of adipose-derived multipotent stromal cells (ASCs), pre-adipocytes, fibroblasts, vascular endothelial cells and immune cells. The regenerative role is played specifically by the SVF and, inside it, especially by the ASCs, by secreting angiogenetic, anti-apoptotic, anti-inflammatory and immunomodulatory growth factors.

Surgeons use different strategies to reconstruct or repair damaged tissues and organs through adipose tissue. Among them, the most effective are the autologous fat transfer and tissue engineering. In the autologous fat transfer, autologous adipose tissue is harvested from one part of the body, purified through some processing techniques and reinjected where necessary. In tissue engineering, some scaffolds made of natural or synthetic materials are used in combination with ASCs and, sometimes, growth factors to repair or reconstruct tissues.

The first experimental part of this doctoral thesis analyzes the *in vitro* performances of one automated closed device and two different disposable kits to process adipose tissue in comparison with the enzymatic digestion, which is the gold-standard technique. All three methods produce micrografts rich of ASCs. Parameters such as ASCs phenotype, viability, growth and replicative rate have been observed.

The second experimental part of this thesis analyzes the *in vitro* and *in vivo* performances of different formulations of hyaluronic acid, a natural and very promising material to regenerate tissues, when combined with ASCs. Parameters such as ASCs viability, interaction with the hyaluronic acid material and adipogenesis have been observed.

# 3. INTRODUCTION

## 3.1. The biology of adipose tissue

Adipose tissue is a connective tissue constituted of adipocytes interspersed with collagen fibers and stromal vascular fraction (SVF), composed of multipotent stromal cells (MSCs), pre-adipocytes, fibroblasts, vascular endothelial cells and immune cells. It plays a central role in lipid storage, cushioning and isolating body and endocrine function, secreting hormones such as leptins and adipokines [1], [2].

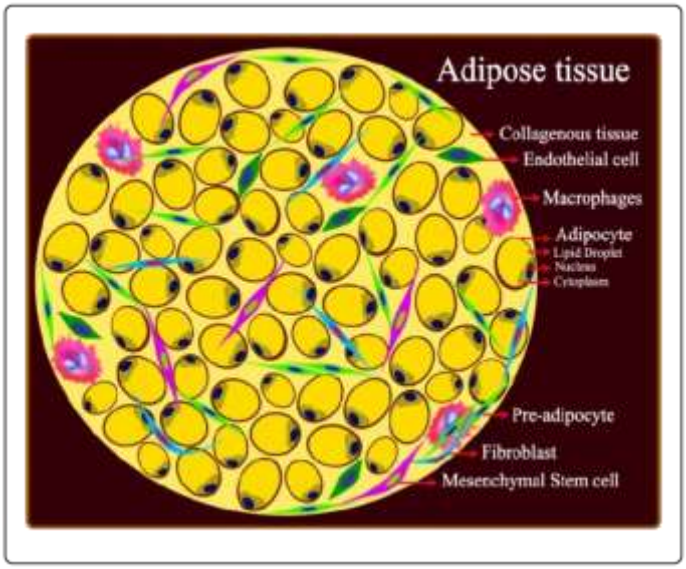


**Fig. 1.** Schematic representation of adipose tissue structure [3].

Adipose tissue can be classified in three groups: white (WAT), brown (BAT) and beige (BeAT). WAT is the most common one. It represents a storage of lipids and source of adenosine triphosphate (ATP) derived from the release of fatty acids during the β-oxidation process. It is also a secretory organ having a high metabolic activity. For instance, it secretes cholesterol, retinol, steroid hormones, prostaglandins and adipokines, like leptin, adiponectin, interleukin-6, tumor necrosis factor-α. Leptin is mainly involved in regulation of energy balance and food intake. Tumor necrosis factor-α is a proinflammatory cytokine. It is responsible of the inflammation, apoptosis, synthesis of interleukin-1 and

interleukin-6 and adipocyte metabolism. It induces insulin resistance. Instead, adiponectin is inversely correlated with obesity. IL-6 is also correlated with obesity and inflammation.

BAT is mainly present in fetuses and newborns and tends to reduce with the growth. In adults, it is only found in limited areas of the body like in the upper trunk. Its main role is thermogenesis. Indeed, its mitochondria express uncoupling protein 1 (UCP1), a protein which stimulates the uptake of lipids and glucose from circulation for thermogenesis. In obese and elderly people, its amount is reduced.

Finally, BeAT has intermediate features between WAT and BAT. Beige adipocytes have multilocular lipid droplets in the cytoplasm and numerous mitochondria. It is visible in the process of differentiation of WAT in BAT, after stimuli, such as cold and exercise [4]–[8].

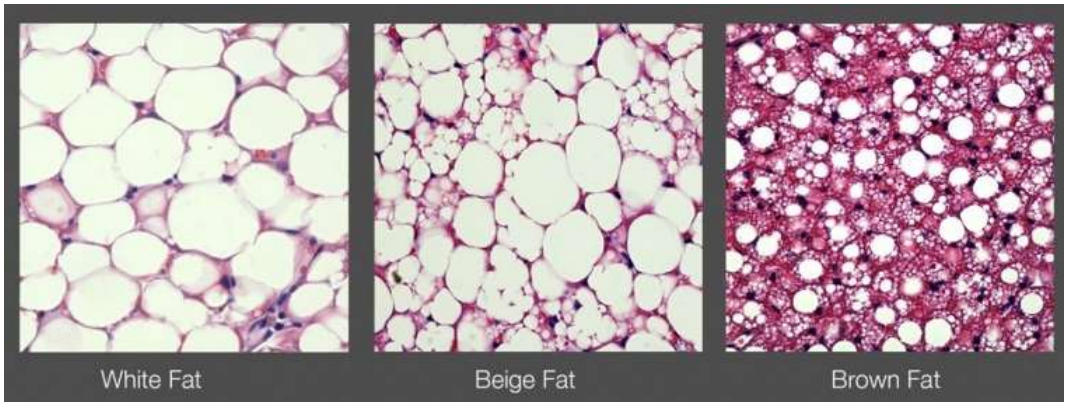


**Fig. 2.** Histology of white, beige and brown adipose tissue [9]

Human adipose tissue can be also classified in visceral (VAT) and subcutaneous (SCAT). VAT, representing around 10% of the total body fat, is present in the abdominal cavity, mainly in the mesentery and omentum and drains directly to the liver. Compared to SCAT, it is more cellular, vascular, innervated and it also contains more inflammatory and immune cells, less preadipocytes and more large adipocytes. VAT is also more metabolic active. [10]

### *3.2. Adipose Stromal Vascular Fraction (SVF)*

Stromal Vascular Fraction (SVF) is an heterogeneous population of mono-nucleated cells, including endothelial cells, fibroblasts, erythrocytes, lymphocytes, macrophages, pericytes and adipose-derived mesenchymal stem cells (ASC). It is made in laboratory from lipoaspirate, enzymatically or non-enzymatically digesting or disrupting it and, then, centrifuging to separate cells from collagen, adipocytes, oil and cellular debris [11].

#### *3.2.1. Multipotent stromal cells (MSCs)*

Multipotent stromal cells (MSCs) are plastic-adherent adult stem cells, which constitute the mesenchymal tissues, such as bone marrow, adipose tissue, amniotic fluid, periosteum and fetal tissues. They were discovered by Friedstein in 1960. They have two important properties: self-renewal and multipotency [12]–[14]. Differently from other stem cells, like IPs and embryonic stem cells, they do not cause teratoma and no ethical or law restrictions on their use is applied [15]. They express specific mesenchymal markers, including CD105, CD90, CD73, CD44, CD29, CD166 and do not express hematopoietic markers, like CD45, CD34, CD14 and CD81. In 2006, the International Society for Cellular Therapy (ISCT) established, as a minimum criteria to define them, their ability to differentiate into cells belonging to the same mesodermal lineage, such as osteocytes, adipocytes and chondrocytes at least *in vitro* [14]. Actually, scientists observed in many cases they can also differentiate into cells of other mesenchymal lineages (i.e. skeletal muscle cells and cardiomyocytes) [16] and also endodermal (i.e. hepatocytes and insulin-producing cells) and ectodermal ones (i.e. neuronal and peripheral glial cells) [17]. In 2007, it was recognized the importance of the perivascular niche for regeneration, the microenvironment in which the cells reside in quiescence until it receives a stimulus of differentiation [18]. The therapeutic and regenerative action of MSCs is due to their release of angiogenetic and anti-apoptotic growth factors. Some example are epidermal growth factor (EGF), vascular endothelial growth factor

(VEGF) and transforming growth factor-beta (TGF-β). Moreover, they release cytokines, like interleukin-6 (IL-6), interleukin-7 (IL-7), interleukin-8 (IL-8), tumor necrosis factor-alpha (TNF-α) with anti-inflammatory and immunomodulatory functions. They mainly act though paracrine mechanisms [19], [20].

#### *3.2.1.1. Adipose-derived stromal cells (ASCs)*

Adipose-derived stromal cells (ASCs) are mesenchymal stem cells first isolated by Zuk in 2002 [21]. They have a similar gene expression profile of the more known bone marrow stromal cells (BMSCs). Indeed, they both express genes involved in homeostasis and tissue repair, such as cytokines and growth factors [22] and differ only in the growth rate, differentiation ability and molecular signature [23]. If compared to BMSCs, their use has some advantages: they can be harvested without invasive procedures, they are around 500 times more abundant and they can be expanded with minimal risk [24], [25].

#### *3.2.1.2. Multipotent stress-enduring stem cells (MUSE)*

Multipotent stress-enduring stem cells (MUSE) are a subpopulation of MSCs, double-positive for the mesenchymal marker CD105 and the pluripotency marker stage-specific embryonic antigen-3 (SSEA-3). They were discovered by Kuroda in 2010. They are known to be pluripotent, or they are able to differentiate into cells belonging to the three germ layers and able to endure stress like oxygen deprivation. They are the main responsible of regeneration and reparation [26]–[28].

# *4. REGENERATION AND RECONSTRUCTION THROUGH ADIPOSE TISSUE*

Adipose tissue has started to be considered not more only a dermal filler but also a regenerative agent after stromal cells have been discovered inside [29], [30].

## *4.1. Autologous fat grafting*

Autologous fat grafting is a surgical technique consisting in a transfer of adipose tissue from one area of the body to another. Autologous fat is an ideal filler, because it is readily available, biocompatible, inexpensive, easily harvestable, do not cause any allergic reactions or rejection. Furthermore, it is rich of ASCs, which have high regenerative capability and paracrine effects. Some of the clinical applications of fat grafting are breast, buttocks and lips augmentation, facial and hands rejuvenation, tissue regeneration (i.e. following scars, wounds and burns) [31], [32] [33].

### 4.1.1. History of fat grafting

Fat grafting after oncological surgery was first introduced by Neuber in 1893. Two years later, Czerny transferred a lipoma to the breast to establish symmetry after a unilateral mastectomy. The technique of liposuction was invented by Fischer in 1975. It consists of a fat removal procedure under anesthesia using blunt cannulas and negative pressure. In 1977, it was used for the first time as a filling product by Illouz. The father of lipofilling was Fourier, who introduced a new technique to infiltrate lipoaspirate. In 1985, Klein described the tumescent technique, also called "wet" method, a liposuction under local anesthesia injected with small cannulas. Specifically, large volumes of a solution constituted by 0.9% NaCl, the vasoconstrictor epinephrine and the local anesthetic lidocaine is administered during the fat harvesting. In 1994, Coleman proposed a less traumatic and

standarized method, consisting of three steps: manual lipoaspiration under low pressure, centrifugation for 3’ at 3400 rpm in 10 ml syringes and reinjection. Through centrifugation, the lipoaspirate can be separed into three different layers: the supernatant layer containing lipids that is poured off, the lower layer containing blood, tissue fluid and anesthetic, which is removed from the syringe and the middle layer constituted by the SVF, which is reinjected in the patient. In 2007, Rigotti treated damages caused by radiotherapy with fat, a process mediated by ASCs. In 2013, Tonnard introduced the concept of nanofat, consisting of an emulsified fat suspension rich of ASCs and lacking in viable adipocytes, which was observed to be useful in skin rejuvination. [29], [30], [34].

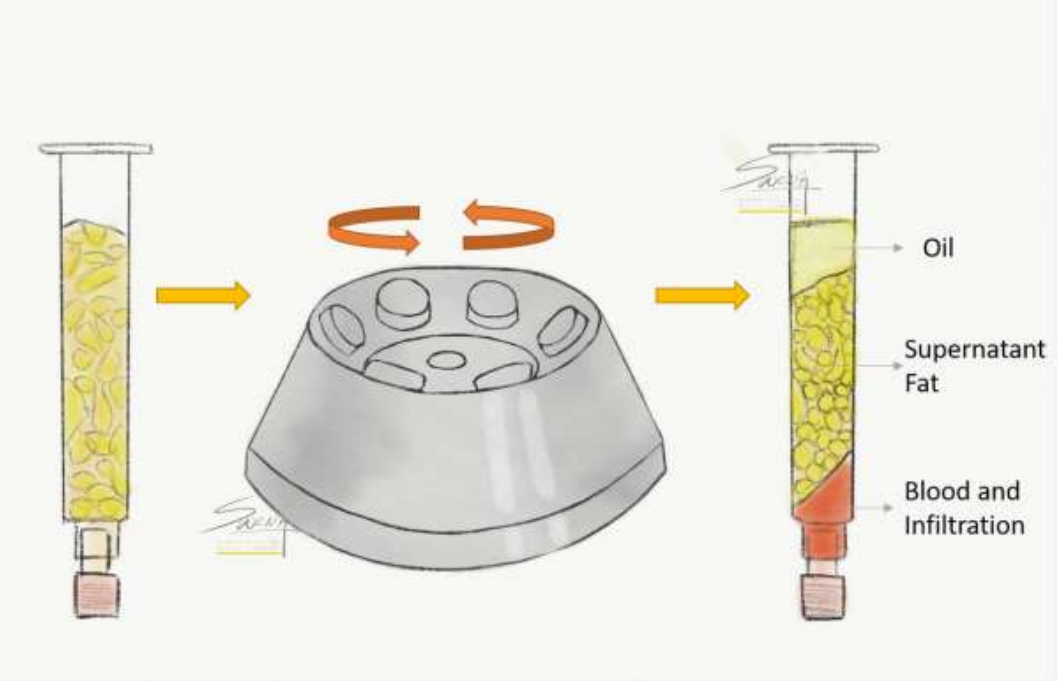


**Fig. 3.** Coleman’s fat grafting after the centrifugation step [35]

### 4.1.2. Complications and limitations

Fat grafting is considered a safe procedure, since the complications are infrequent. However, the most common ones relative to the donor-site are haematoma, swelling, paraesthesia, pain and hypertrophic scarring. On the contrary, the complications in the recipient-site include infection, fat necrosis, calcification and

oil cyst formation. The reabsorption rate, ranging between 20 and 90%, represents also an important issue, since, so far, the outcomes of fat grafting can be hardly predicted. Indeed, they are influenced by a too large number of variables depending on the technique, but also on patient factors, such as the smoking habit and anticoagulant therapies. Finally, another limitation is that the feasibility of the fat graft procedure is linked to the amount of adipose tissue available in the patient [30], [34], [36].

### 4.1.3. Cell-assisted lipotransfer (CAL)

A recent procedure was introduced to improve the graft viability and limit the resorption rate. It is named cell-assisted lipotransfer (CAL) and it consists in fat grafting enriched with SVF cells. However, the improved outcomes were observed only for small volume of fat (<100 mL) and this technique seems not to be completely devoid of risks and to not reduce the number of surgical procedures needed after the first fat graft. Therefore, CAL efficacy and especially safety are still matters of debate and would require further clinical studies [32], [37]–[39].

### 4.1.4. Platelet-rich plasma (PRP)

Platelet-rich plasma (PRP) is another method to increase the graft viability. It consists in a small amount of plasma concentrated of autologous platelets, which are rich in growth factors. Also PRP efficacy and safety are still controversial [40]–[43].

### 4.1.5. Fat grafting technique

Fat grafting is constituted by three steps: harvesting, processing and reinjection.

#### *4.1.5.1. Fat harvesting*

Less traumatic techniques are generally preferred because they better preserved the adipocytes viability and graft survival. Usually, adipose tissue is harvested though aspiration and vacuum-assisted, water-assisted, or ultrasound-assisted lipectomy. A higher graft viability and a lower fibrosis were observed using low-pressure techniques. Moreover, cell viability is better preserved with larger cannulas. Commonly, a tumescent solution such as a vasoconstrictor are used. The most frequent local anesthetic is lidocaine [44], [45].

#### *4.1.5.2. Fat processing*

The reason of fat processing is to eliminate contaminants, including cellular debris, oil, dead cells, collagen fibers and erythrocytes from lipoaspirates, in order to avoid inflammation and, thus, poor graft retention. Furthermore, it allows to optimize the number of ASCs, that, according some theories, improves graft viability. The processing methods can be classified into two big groups:

1. Enzymatic methods
2. Non-enzymatic methods

Figure 4 briefly summarizes the pros and cons of enzymatic and non-enzymatic methods.

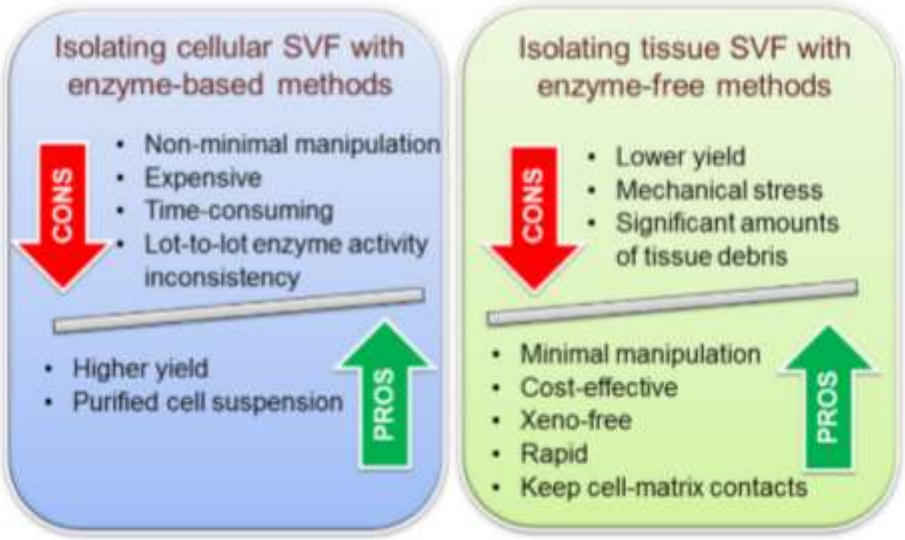


**Fig. 4.** Comparison between enzymatic and non-enzymatic method to isolate the SVF [46].

#### 4.1.5.2.1. Enzymatic methods

Enzymatic methods like using collagenase or trypsin are the gold-standard ones in the laboratory. The final products are the cells. They are very efficient, but the whole ASCs isolation procedure is time-consuming and expensive. Although slight differences among the protocols, they are generally constituted by a fat washing step, incubation with the enzyme, centrifugation to separate cells from the oil and the enzyme, erythrocytes lysis, another optional washing step and cell culture and expansion. Moreover, the use of enzymes is forbidden in clinical practice. Indeed, according to Good Manufacturing Practice regulations of the European Parliament and Council (EC regulation no. 1394/2007), only minimal cell manipulation is allowed in clinical setting. Indeed, the original biological, physiological and structural characteristics of cells and tissues cannot be modified. Enzymes substantially manipulate tissues disrupting the cell-cell interactions and cleaving some cell membrane receptors [47]–[50].

#### 4.1.5.2.1.1. Mechanical methods

The most common fat processing mechanical methods are: centrifugation, filtration, washing in physiologic solutions, decantation, Telfa rolling, emulsification.

They can be performed manually or through automated devices.

#### 4.1.5.2.1.2. Manual methods

According to various studies, the ideal fat processing technique should fulfill these requirements:

1) to preserve the maximum number of intact adipocytes. They are responsible of the graft volume and survival.

2) to remove the maximum number of contaminants, including the unnecessary fluid volume, blood and lipids in order to avoid inflammatory cytokines release and fat graft resorption over time.

3) to preserve the maximum number of MSCs. In fact, these cells are responsible of angiogenesis and regeneration. [13]

Unfortunately, none of the mechanical techniques fully possesses each of these characteristics and therefore none is uniformly recognized by the scientific community as the best one.

Different studies have been performed in order to evaluate the safety and efficacy of mechanical methods. Some of them compare the results achieved from different methods. In the following tables, the main general and histological features of the different methods are summarized:

| General features | | | | | |
|---|---|---|---|---|---|
| **Method** | | **Pros** | | **Cons** | References |
| **Centrifugation** | ✓ | Collection of a great number of mesenchymal stem cells | ✓ | Disruption of adipocytes | [51]–[58] |
| | ✓ | Optimal removal of contaminants | | | |
| **Filtration** | ✓ | Good removal of contaminants | | | [52], [53], [57] |
| **Washing** | ✓ | Collection of a modest number of mesenchymal stem cells | ✓ | Reduction of adipocytes number | [52]–[55], [57] |
| **Decantation** | ✓ | Adipocytes preservation | ✓ | Poor removal of contaminants | [52], [54], [57] |
| **Telfa-rolling** | ✓ | Collection of a great number of mesenchymal stem cells | ✓ | Quite labor intensive and more suitable for small areas | [51]–[53], [58] |
| | ✓ | Optimal removal of contaminants | | | |
| | ✓ | Adipocytes preservation | | | |
| **Emulsification** | ✓ | Collection of a great number of mesenchymal stem cells | ✓ | Significant reduction of adipocytes number | [46] |

**Fig. 5.** Pros and cons of the different mechanical methods: general features.

| Histological evaluation | | | |
|---|---|---|---|
| **Methods** | **Pros** | **Cons** | **References** |
| **Centrifugation** | ✓ High volume retention<br>✓ Low viability | ✓ Possible areas of fibrosis and calcification | [51]–[58] |
| **Filtration** | ✓ High viability | | [52], [53], [57] |
| **Washing** | ✓ High viability<br>✓ High vascularity | | [52]–[55], [57] |
| **Decantation** | | ✓ Low volume retention<br>✓ Severe cists<br>✓ Low fat graft viability | [52], [54], [57] |
| **Telfa-rolling** | ✓ High volume retention | | [51]–[53], [58] |
| **Emulsification** | ✓ High viability<br>✓ High vascularity | | [46] |

**Fig. 6.** Pros and cons of the different mechanical methods: histological evaluation.

As shown in table 5, decantation preserves an high number of viable adipocytes. However, it does not remove enough contaminants, resulting in low graft viability. Telfa rolling produces a fat graft free of contaminants, with a higher number of alive ASCs, with high graft retention. However, this technique is time-consuming and, therefore, can be used only for small areas. Centrifugation is the most widely used method for fat processing. It removes contaminants and preserve ASCs, but disrupt the adipocytes. However, low centrifugation speeds better preserve the adipose tissue integrity and the cell viability and differentiation potential. Washing is generally considered a good technique, since it preserves a large number of both ASCs, but the number of adipocytes is reduced. Finally, filtration is an efficient method since it eliminates contaminants and maintains viable adipocytes and a large portion of ASCs. Also considering the histological evaluation, as shown in table 6, filtration and washing seem to be the best techniques since the viability is preserved and no fibrosis, calcification or cists are visible [52], [56], [58]–[60].

#### 4.1.5.2.1.3. Closed devices and single-use kits

The advantage of the use of closed automated devices is that they can perform perfectly standardized processes, do not require specific skills and, in addition, they guarantee the sterility. This last characteristic is also preserved even if the device requires the operator manual skills, but reproducibility is surely lower. Recently, a large plethora of devices and disposable kits have been patented and commercialized. Some of them make use of enzymes, whereas others use mechanical methods. For instance, Celution® 800/CRS (Cytori Therapeutics, USA), Sepax® 2 (Biosafe SA, Italy), Stempeutron® (Stempeutics Research, India), Unistation® (NeoGenesis, South Korea) and Icelletor® (Tissue Genesis, USA) belong to the first group. Revolve® (GD Medical Pharma, Netherlands), Lipogems® (Lipogems International SpA, Italy), Rigenera® (Human Brain Wave,

Italy), Puregraft® (Cytori Therapeutics, USA), StromaCell® system (MicroAire Aesthetic, USA) belong to the second group. Puregraft® (Cytori Therapeutics, USA) and Revolve® (GD Medical Pharma, Netherlands) are based on filtration and washing, Lipogems® is based on filtration and beads microfracture, StromaCell® system is based on centrifugation, Rigenera® is based on microfracture.

Generally, automated devices have been demonstrated giving better results than manual methods. [61]

| **Puregraft®** | **Revolve®** | **Lipogems®** | **StromaCell®** |
|---|---|---|---|
|  |  |  | 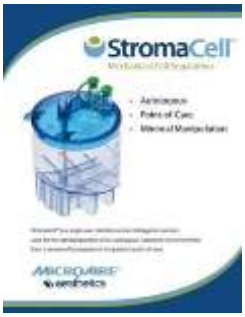  |

**Fig. 7.** Some exempla of closed devices, which do not make use of enzymes.

#### *4.1.5.3. <u>Fat delivery</u>*

Fat injection represents the crucial step of the whole process. The best results were obtained when the recipient-site vascularity was good. Fat injection can be executed using blunt or sharp cannulas, in absence or presence of fibrosis, respectively. Indeed, fibrosis needs to be removed to avoid damage to other anatomical structures. Small-gauge cannulas are less traumatic toward the recipient site.

Usually, small amount of fat are injected to avoid resorption, to preserve the graft viability and to allow integration with the surrounding recipient site. A good distribution of fat is also important to avoid accumulation.

### 4.1.6. How does the fat grafting occur?

Different theories about the fat grafting mechanism have followed each other over time. For instance, Peer described the "graft survival theory", which supports the fat graft survival until neovascularization in the recipient site. On the contrary, Eto proposed the "graft replacement theory", asserting that three different zones can be identified from the periphery to the centre of the graft: an area in which adipocytes survive, an area of regeneration in which adipocytes dies and are replaced by new ones differentiated from ASCs and an area in which both adipocytes and ASCs die. Finally, Neuhof and Hirshfeld described the "host cell replacement theory", which states that all the donor-site adipocytes die and are replaced by recipient-site cells. Most probably, all these theory contribute to correctly explain the mechanism. Briefly, adipocytes survive if the transplantation site is well vascularized and attract the recipient cells, which also contribute to regeneration through paracrine stimuli and structural support, as well as the injected SVF cells present in the fat graft. [36]

### 4.1.7. Characterization of ASCs-rich micrografts obtained from different devices

#### *4.1.7.1. General introduction*

In this chapter, one closed automated device, based on mechanical disaggregation and filtration, named Rigenera® and two disposable manual kits, based on filtration and emulsion, named Hy-Tissue SVF® and Hy-Tissue Nanofat® have been tested *in vitro*. Specifically, parameters such as cell phenotype, viability and replication rate have been observed. They have been analysed separately and their results have been always compared with the gold-standard enzymatic method. In the general conclusion, in the end of this chapter, only a brief comparison between the three methods is presented, because, unfortunately, experiments referring to the three techniques were executed following different timetables and protocols.

#### *4.1.7.2. Rigenera® (Human brain Wave, Turin)*

##### 4.1.7.2.1. Introduction

Rigenera® is a closed automatic device for tissue processing composed by an engine and disposable sterile capsules. It mechanically disaggregates the tissue though steel blades rotating at 80 r.p.m. Afterwards, the product of disaggregation is filtered through pores of 70-80 μm. It has many advantages, such as it is non-invasive, rapid and easy to use, automatic and, therefore, standardized, sterile and safe and the process is completely autologous. The utilization fields are many: esthetic surgery [62], dermatology [63], [64], vulnology [65], [66], orthopedics [67], [68], odontostomatology [69], [70] and in the heal of the androgenetic alopecia [67], [71]

The general aim of the present study was to deeply analyze the efficacy of the Rigenera® procedure *in vitro*.

Specifically, three objectives have been pursued:

1. Method optimization. The best processing timing among 30'', 45'' and 60'' was established
2. Comparison with the gold-standard collagenase digestion
3. Comparison between two different harvesting sites: thigh and abdomen.

**Fig. 9.** Rigenera® capsule and device.

#### 4.1.7.2.2. Material and methods

##### 4.1.7.2.2.1. Adipose tissue samples collection

Adipose tissue was harvested by 9 women subjected to liposuction, aging between 41 and 69 years old. Patients signed the informed consents before the tissue collection. The water-assisted liposuction named BEAULI® protocol was used. It is described in detail in [72].

##### 4.1.7.2.2.2. Cell isolation and culture

Each adipose tissue sample was divided in 2 portions. 4 mL of lipoaspirate were placed in a Rigenera® capsule and other 4 mL of complete culture medium Dulbecco Minimum Essential Medium (DMEM) (Sigma-Aldrich, Italy) containing 10% of Fetal Bovine Serum (FBS), 1% of a mix of penicillin/streptomycin 1:1 (GIBCO Life Technology, Italy) and 0.5 % amphotericin B (GIBCO Life Technology, Italy) were added. The Rigenera® device was operated for 30'', 45''

or 60''. The collected SVF was withdrawn from the capsule by a syringe, filtered through a 70-µm nylon mesh and centrifuged at 3000 rpm for 7'. The supernatant was discarded and SVF was resuspended in 6 mL of complete medium, plated in a 25 cm2 flask (BD FalconTM, Becton Dickinson, Italy) and incubated at 37°C and 5% CO2. The second portion of lipoaspirate was digested with collagenase following the collagenase protocol, as reported in [23]. Briefly, 4 mL were digested with 1 mg/mL type I collagenase (GIBCO life technology, USA) in Hank's Balanced Salt Solution (HBSS) and 2% bovine serum albumin (BSA) at 37°C for 45'. The enzymatic action was neutralized adding complete medium. Then, the sample was centrifuged at 3000 rpm for 7', the supernatant was discarded and the SVF pellet was incubated with 3 mL of 160 mM NH4Cl at room temperature for 10' to lyse the erythrocytes. After centrifugation, the SVF was resuspended in 6 mL of complete medium, filtered through a 70-µm nylon mesh, plated in a 25 $cm^2$ flask with complete culture medium and incubated at 37°C and 5% CO2. The medium was first changed after 72 hours and, successively, every 24 hours. At confluence, cells were detached incubating them with trypsin-EDTA 1% (GIBCO Life Technology, USA) at 37°C for 5' and re-plated in a 75 $cm^2$ flask.

**Fig.10.** Rigenera® procedure.

#### 4.1.7.2.2.3. Morphological analysis and cell viability test

At confluence, the cells were observed under a light microscope (Optika Microscopes Italy) furnished with a Leica camera at 20x magnification. Pictures of cells obtained with the three different Rigenera® operating timings, enzymatic method and from the two different harvesting sites were taken.

Cell viability and growth rate were evaluated by the cell viability test with trypan blue exclusion method. Cell suspension and trypan blue were mixed 1:1. The solution was put in a Bürker chamber and cells were counted under a light microscope at 20x magnification, excluding the blue non-viable cells. The growth rate was determined by the growth curve.

#### 4.1.7.2.2.4. Immunophenotyping

At confluence, the cells were detached with trypsin-EDTA. Around 200000 cells were placed in each Eppendorf tube. The pellet was washed with 1 mL of 1% FBS in PBS and then labelled with fluorescent-dye conjugated antibodies in a final volume of 100 µL of 1% FBS in PBS and incubated for 30' in ice. The herein examined antibodies were: APC-conjugated CD90 (dilution 1:5), PerCP-Cyt5.5-conjugated CD105 (dilution 1:20), BV421-conjugated CD73 (dilution 1:20); BV785-conjugated CD44 (dilution 1:20), PE-conjugated CD34 (dilution1:5), FITC-conjugated CD29 (dilution 1:20), BV650-conjugated CD45 (dilution 1:20). All the antibodies were purchased from BD Biosciences, Becton Dickinson Italy S.p.A., Milan. Alexa Fluor-488-conjugated SEEA3 (dilution 1:20) was purchased from Aurogene S.R.L, Rome. After the incubation, the pellet was rinsed, resuspended in 300 µL of 1% FBS in PBS and transferred in flow cytometry tubes. The immunophenotyping was performed through a FACS canto II (BD, Becton Dickinson, Italy).

#### 4.1.7.2.2.5. Statistical analysis

Data were expressed as mean ± standard deviation. Unpaired samples student's t-tests were performed and differences between two groups were considered statistically significant, when $p\text{-value}<0.05$.

#### 4.1.7.2.3. Results

##### 4.1.7.2.3.1. Rigenera® method optimization

In order to determine the best processing timing among 30'', 45'' and 60'', in terms of number of ASCs and growth rate, the cell viability test and microscopic analysis were performed. First, the cells were counted at passage 0 (fig. 10). Due to the strong presence of erythrocytes, at this level, the count of ASCs results not to be reliable. However, a first datum can be derived: the number of cells with 60'' treatment was much higher than with 45'' and 30'' (data shown in the table, fig. 10). After one week, only cells capable of forming fibroblast-like colonies, attached to the flask and were countable. The number of ASCs collected from thigh was almost three times higher with the 60'' treatment than with the 45'' and 18 times higher than with the 30'' one. In addition, the mean time of confluence resulted to be 8 days lower with 60'' treatment than with the 45'' and 30'' treatment. The number of ASCs collected from abdomen was two times higher with the 60'' treatment than with the 45'' and almost 5 times higher than with the 30'' one and the mean time of confluence was 7 days lower with 60'' treatment than with the 45'' and 30'' treatment. Therefore, 60'' can be considered the most efficient timing. (fig. 10).

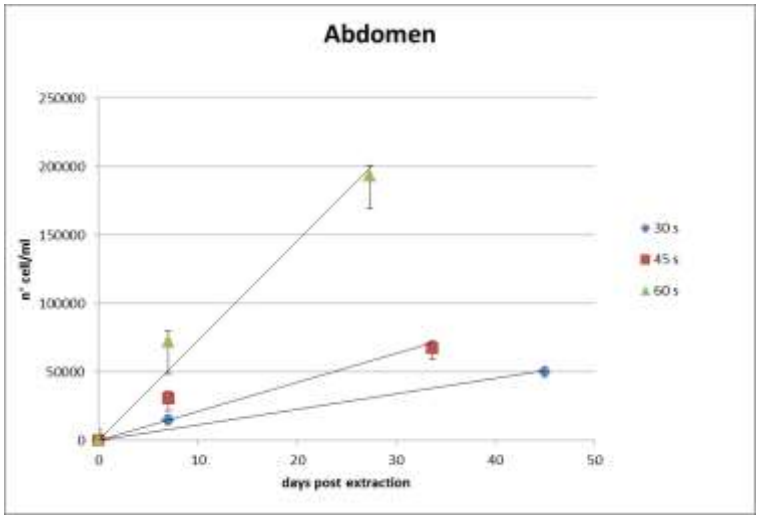


| **Abdomen** | Cell number p0 $10^6$ ± SD | Mean $10^5$cells/ml (after 1week) ±SD | Mean time of confluence | Mean $10^5$ cells/ml (at confluence) ±SD | Mean $10^5$ cells/ml growth per day | % of cell growth |
|---|---|---|---|---|---|---|
| Rigenera 30 s | 4,133±0,33 | 0,147± 0,05 | >45 | <0,5 | 1,134 | 2.43 |
| Rigenera 45 s | 6,84±0,19 | 0,305± 0,09 | 34±6,5 | 0,677±0,15 | 2,107 | 4.52 |
| Rigenera 60 s | 15,16±0,49 | 0,722± 0,13 | 27±3,7 | 1,93±4,20 | 7,272 | 15.61 |

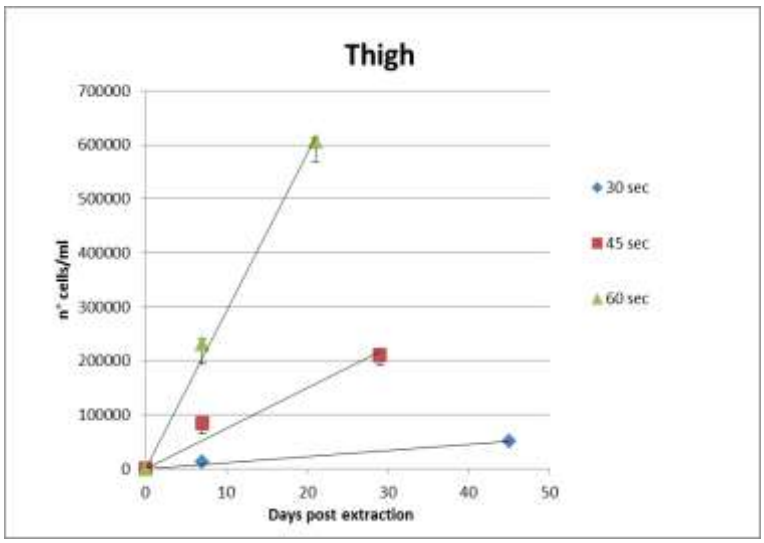


| **Thigh** | Cell number p0 $10^6$ ± SD | Mean $10^5$cells/ml (after 1week) ±SD | Mean time of confluence | Mean $10^5$cells/ml (at confluence) ±SD | Mean $10^5$ cells/ml growth per day | % of cells growth |
|---|---|---|---|---|---|---|
| Rigenera 30 s | 7,2±0,28 | 0,127± 0,05 | >45 | <0,5 | 1,127 | 0.17 |
| Rigenera 45 s | 9±0,35 | 0,842± 0,04 | 29±1,4 | 2,10±0,33 | 7,488 | 1.13 |
| Rigenera 60 s | 21±0,16 | 2,320± 0,14 | 21±1,4 | 6,05±0,64 | 29,237 | 4.41 |

**Figure 10. Rigenera® method optimization.** Cell viability test with trypan blue exclusion method. At passage 0, the number of total cells was much higher with the 60'' Rigenera® treatment compared to the other timings (data shown in the table). After one week, the number of the pure ASCs was still higher with the 60'' Rigenera® treatment in both thigh and abdomen.

ASCs images in fig. 11 clearly represent the number, disposition and cell morphology. Cells, seeded in flasks, formed clusters, thus high and low density regions were both present. Rigenera® treatment did not affect the cell morphology. Indeed, no signal of sufferance was observable and the membranes and the nuclei were preserved. The number of ASCs appeared lower after the 30'' and 45'' treatments compared to the 60'' treatment.

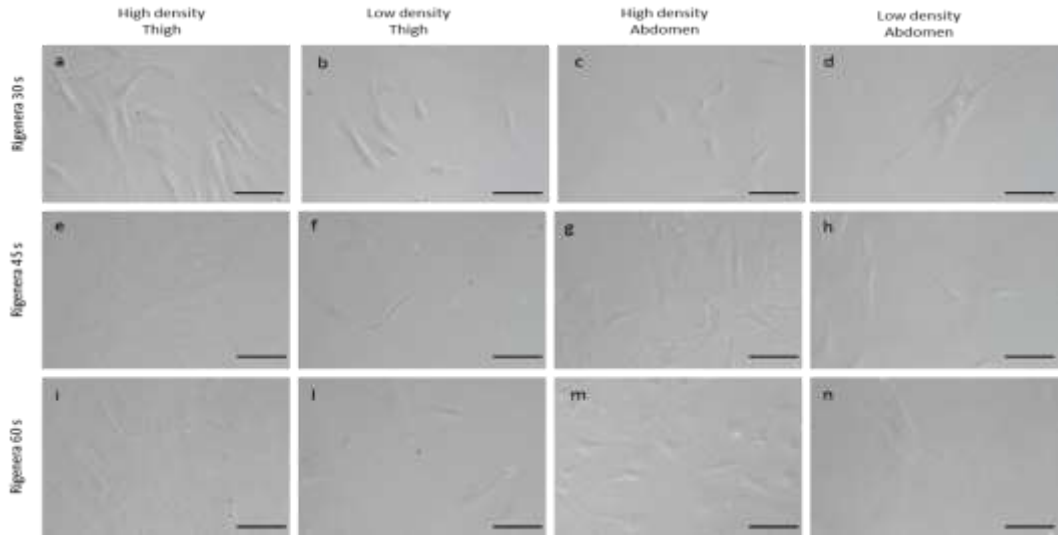


**Fig. 11. Rigenera® method optimization (2)** Microscopic images (10x) of ASCs from thigh (columns 1-2) and abdomen (columns 3-4). They were obtained from Rigenera® operating at different timings: 30'' (raw 1), 45'' (raw 2) and 60'' (raw 3). High (column 1-3) and low (column 2-4) density regions are both present. The morphology looks unaltered for all the treatments.

#### 4.1.7.2.3.2. Comparison between Rigenera® and the enzymatic method

After one week of culture, the number of ASCs collected with enzymatic method was almost two times higher than with Rigenera® for thigh and four times higher for abdomen. Therefore, they took a shorter time to reach the confluence (fig. 12).

However, at high passages (i.e. 10), no statistically significant difference in number was observed (fig. 13). To determine it, a p-value test between the two groups was performed and the p-value resulted higher than 0.05. It means that at this level the growth rate was comparable. Fig. 14 shows that the ASCs morphology obtained with Rigenera® and enzymatic method is similar even at high passages.

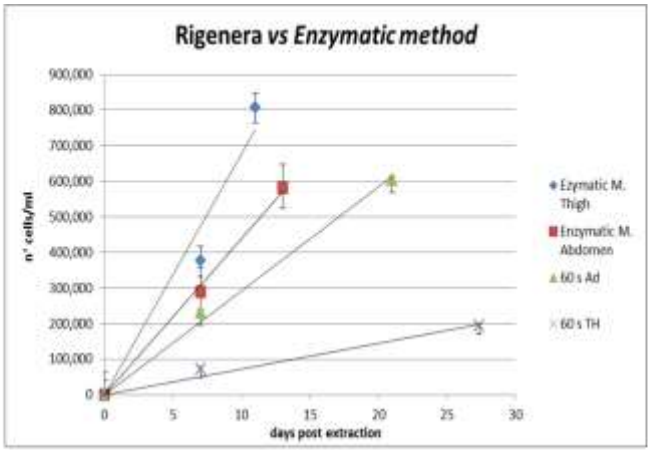


| | Mean $10^5$ cells/ml (after 1week) ±SD | Mean time of confluence | Mean $10^5$ cells/ml (at confluence) ±SD | Mean $10^5$ cells/ml growth per day | % of cells growth |
|---|---|---|---|---|---|
| **Enzymatic M. Thigh** | 3,760± 0,71 | 13±3,5 | 8,07±0,75 | 67,710 | 100 |
| **Rigenera 60 s Thigh** | 2,320± 0,14 | 21±1,4 | 6,05±0,64 | 29,237 | 43 |
| **Enzymatic M. Abdomen** | 2,890± 1,10 | 12±2,30 | 5,81±0,98 | 46,591 | 100 |
| **Rigenera 60 s Abdomen** | 0,722± 0,13 | 27±3,7 | 1,93±4,20 | 7,272 | 15.61 |

**Fig. 12.** Comparison between Rigenera® and the enzymatic method. Growth rate comparison between ASCs from Rigenera® and enzymatic method. ASCs harvested from the last one growed more rapidly.

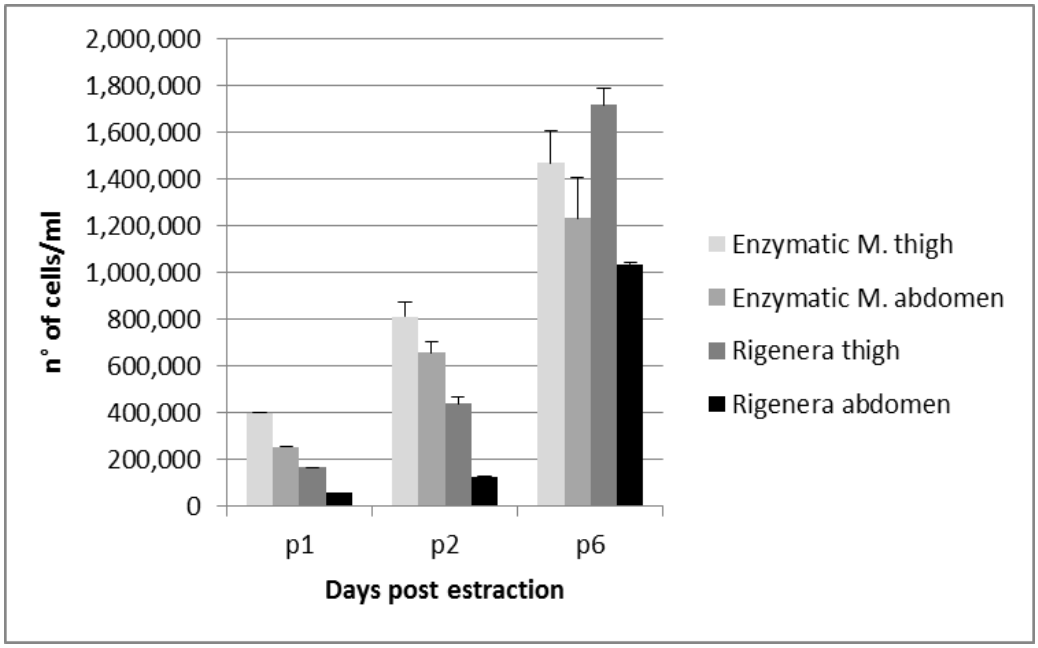


**Fig. 13.** Comparison between Rigenera® and the enzymatic method (2). Growth rate and microscopic images of ASCs. The histogram shows the ASCs number from thigh and abdomen with Rigenera® and collagenase method at passages 2 (p2), 6 (p6). At low passages (p2 and p6), the differences between Rigenera® and collagenase method are significant ($p<0.05$). These differences become not significant at higher passages (p10) ($p>0.05$), thus the growth rate becomes comparable.

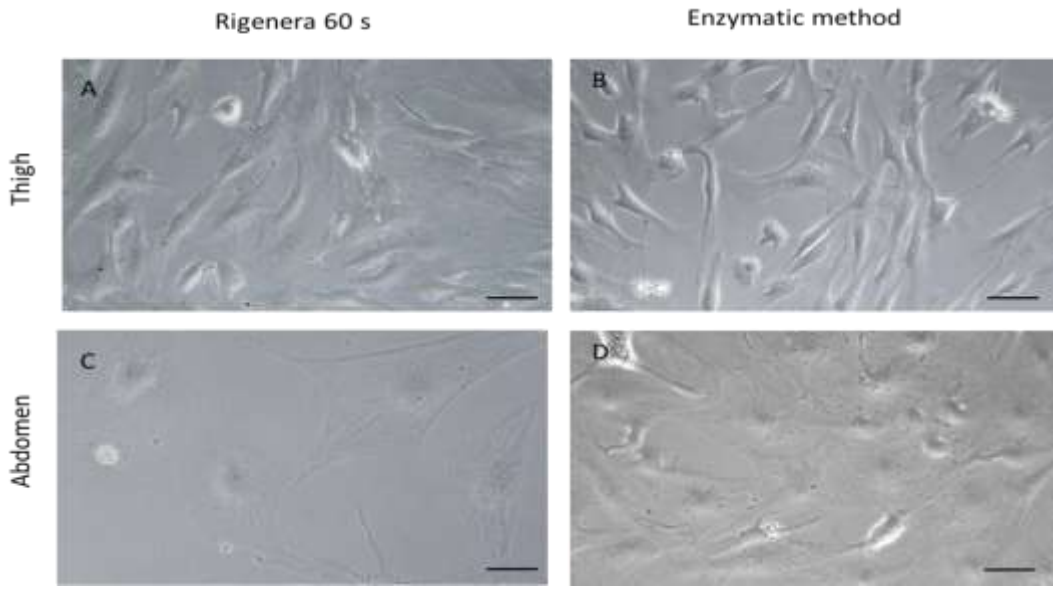


**Fig. 14.** Comparison between Rigenera® and the enzymatic method. The microscopic images demonstrate that the phenotype does not change at high passages (p10).

The immunophenotypic analysis at p0 confirmed the much higher yield of ASCs for enzymatic method (12.7% of ASCs from thigh and 4.36% of ASCs from abdomen) (fig.15) compared to Rigenera® (0.92% of ASCs from thigh and 0.15% of ASCs from abdomen) (fig. 16). Specifically, single antigens or combinations of two antigens were tested. As the ASCs isolated by the gold-standard method, they strongly express CD105, CD90, CD73 and CD29 and do not express the haematopoietic marker CD45. Instead, a different expression of the haematopoietic marker CD34 was observed between the two techniques. Indeed, this antigen was higher expressed after collagenase digestion, probably meaning that Rigenera® method allowed isolating a purer cell population. At higher passage (p10), the antigens pattern was similar, confirming the phenotype maintenance. We also identified a generally low presence of the Multi-lineage differentiating stress enduring cells (MUSE cells), an interesting subpopulation of ASCs, double-positive for CD105 and SSEA3, which are stress-tolerant, non-tumorigenic, pluripotent (they can differentiate into cells of the three germ layers) and with the ability of tissue repair [12–14].

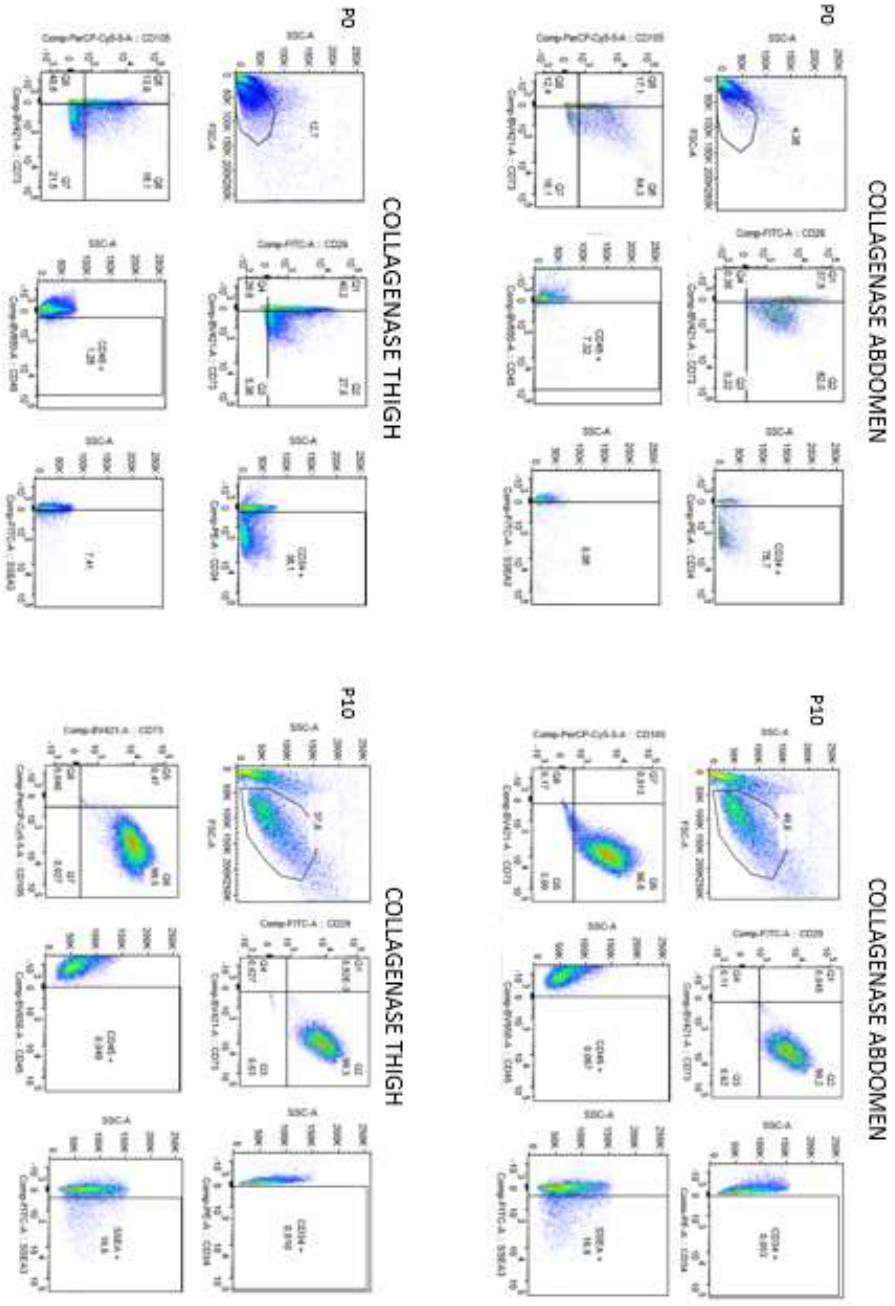


**Fig. 15.** Flow cytometry after collagenase digestion. Immunophenotyping analysis of ASCs from abdomen and thigh at passages 0 and 10 obtained from collagenase digestion.

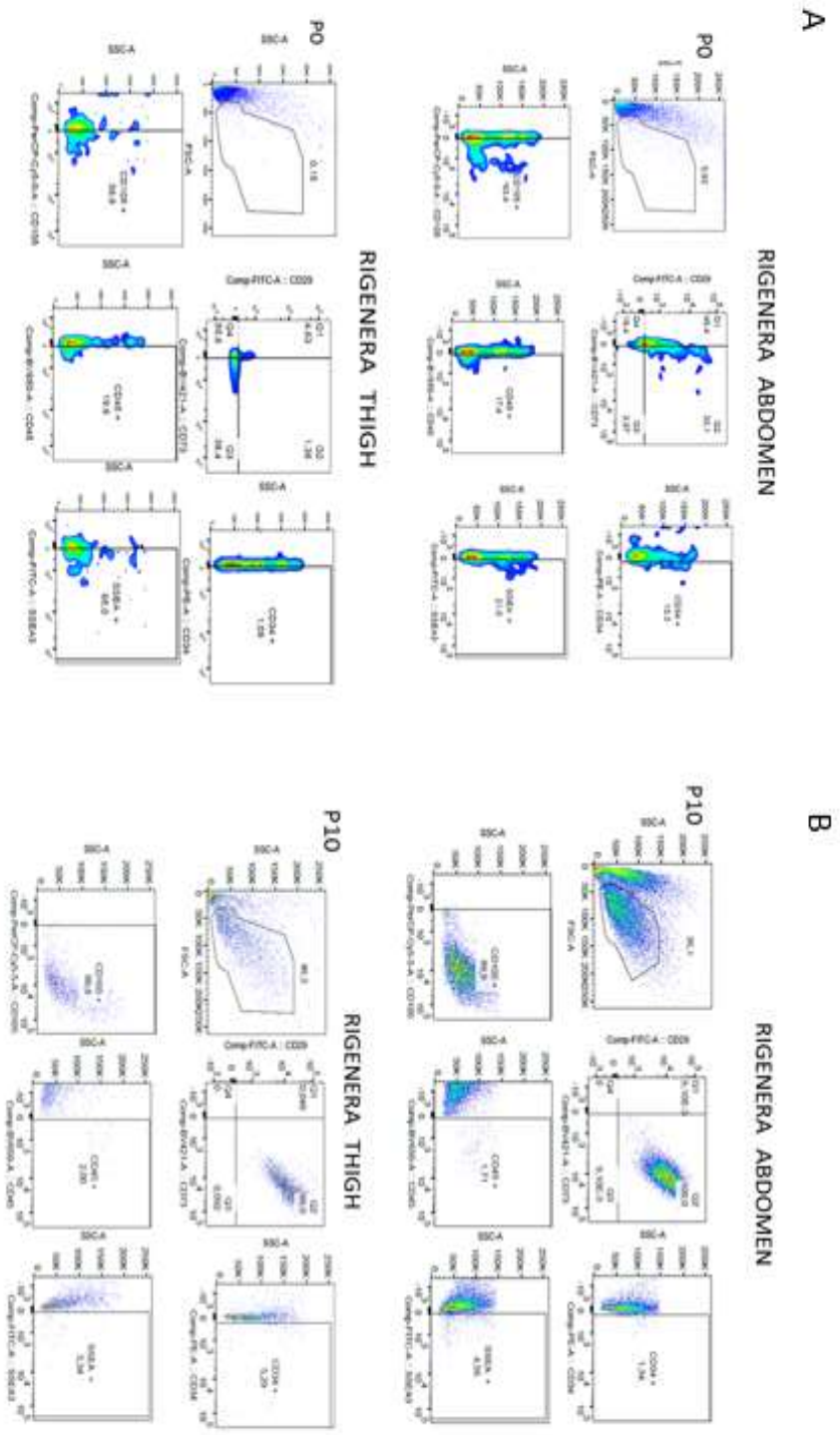


**Fig. 16.** Flow cytometry after Rigenera® processing. Immunophenotyping analysis of ASCs from abdomen and thigh at passages 0 and 10 obtained from Rigenera® method. The marker expression profile was comparable to the one of ASCs from collagenase and preserved over passages.

#### 4.1.7.2.3.3. Comparison between thigh and abdomen

From microscopic analysis, a first difference between thigh and abdomen was detectable: cells from abdomen were less abundant and grow more slowly. In addition, the morphology was slightly different: they are more flattened and spreaded. (fig.15) From the cell count, ASCs obtained from thigh resulted three times more abundant than ASCs from abdomen and they reached the confluence 6 days before (fig.13). However, the differences were not statistically significant after a long period of culture and many passages. (i.e. 10) ($p>0.05$) (fig.14) The immunophenotypic analysis showed that the surface marker expression profile between ASCs from thigh and abdomen was comparable and preserved over time. (fig.14).

### 4.1.7.2.4. Discussion

The enzymatic method, which has been used for 40 years in the laboratory in order to isolate cells, although to be the best, is definitely not compatible with clinics, due to the long-lasting procedure and to the laws restrictions. Furthermore, it destroys the stem-cell niche, that microenvironment, which surrounds the stem cell, allowing interactions with the neighbouring ones and promoting cell survival, proliferation and differentiation. Many efforts have been done to establish a mechanical method having a yield comparable to the one of collagenase. Unfortunately, so far, none of them has the same performance. In addition, in order to use it in vivo, a closed device is needed and the method has to be fast, safe, standardized and autologous. Rigenera® reply to all this requirements. Herein, we optimised the Rigenera® operating timing demonstrating that the best one is 60'. We also proved that Rigenera® treatment does not affect the cell morphology, since the cell appearance under microscope was not altered and was also preserved over time (passages higher than the ninth). Unfortunately, the cell yield and thus, the mean time of confluence, was lower, but the replication rate was comparable at higher passages

(from the tenth passage). The antibody expression of the typical mesenchymal stem cell markers (CD105, CD90, CD73, CD44 and CD29) and the haematopoietic markers (CD45 and CD34) was similar to collagenase method and preserved over time. Thus, no alteration in the ASCs phenotype was observed. An average expression of MUSE SSEA3 antigen was also detected. Surgeons commonly harvest adipose tissue from thigh and abdomen. We demonstrated that the ASCs yield from thigh was higher, such as the cell replicative rate, which however became very similar at high passages (passages higher than the tenth one). On the contrary, the marker expression was very similar, also over time. This should lead surgeons to prefer thigh as a harvesting site, whenever possible.

#### 4.1.7.2.5. Conclusion

The efficacy of the enzymatic method is well-known, but the procedure time is not compatible with the clinics and it is forbidden by the law.

Herein, we demonstrated that Rigenera® can be a valid clinical alternative, since, although the yield is lower, the cell phenotype is preserved, also over time, such as the ASCs replication rate.

Furthermore, we showed that the thigh is a preferable harvesting site compared to the abdomen, due to the higher ASCs yield having better replicative rate.

Our future perspective will be to better characterize, through biomolecular analysis, both the final product of Rigenera® and the ASCs at passage 1. In particular, in order to further validate Rigenera® method, we aim to determine the expression level of genes involved in stemness, adipogenic, osteogenic and chondrogenic differentiation, angiogenesis, inflammation and cell aging.

#### *4.1.7.3. Hy-tissue SVF® (Fidia Farmaceutici, Abano Terme, Padua, Italy)*

##### 4.1.7.3.1. Introduction

Hy-tissue SVF® is a disposable kit constituted by a 250 mL homogenization bag with a 120 µm filter and a Teflon insert, 20 mL removable plunger syringes and syringe caps. The syringe is screws to the bag and the lipoaspirate is injected inside, homogenized by massaging for 4' and aspired though another syringe. Then, the product of homogenization is centrifuged at 400 g for 10'' [73].

The general aim of the present study was to deeply analyze the efficacy of the Hy-tissue SVF® procedure *in vitro* and the results were compared with the gold-standard collagenase digestion.

**Fig. 17.** Hy-Tissue SVF® device [73].

#### 4.1.7.3.2. Material and methods

##### 4.1.7.3.2.1. Adipose tissue samples collection

Adipose tissue was harvested by 11 women subjected to liposuction, aging between 43 and 65 years old. Patients signed the informed consents before the tissue collection. The water-assisted liposuction named BEAULI® protocol was used. It is described in detail in [72].

##### 4.1.7.3.2.2. Cell isolation and culture

Each adipose tissue sample (35 mL) was divided in 2 portions. 5 mL of lipoaspirate were digested with collagenase following the collagenase protocol, as reported in [23]. The remaining part was processed with the Hy-Tissue SVF® device. Specifically, the solution, which exit before massaging (the Klein discard solution) was collected in a 50 mL tube separately from the product obtained after massaging (post-massage). All the samples were centrifuged at 3000 rpm for 7'. By this step, the pellets were separated from the condensed fat. The condensed fat was enzymatically digested and the obtained cells were counted and cultured. Instead, the pellets were incubated with 10 mL of Red Blood Cell Lysis Solution (Miltenyi Biotec, Germany) for 10' at room temperature, to lyse the erythrocytes. For the Fibloblastic-Colony-Forming Unit (CFU-F) assay, 3000 cells were resuspended in 2 mL of complete medium, plated in a 6-well plate (BD FalconTM, Becton Dickinson, Italy) and incubated at 37°C and 5% CO2. Other 10000 cells were resuspended in 6 mL of complete medium, plated in a 25 cm2 flask (BD FalconTM, Becton Dickinson, Italy) and incubated at 37°C and 5% CO2. The media were first changed after 72 hours and, successively, every 24 hours. At confluence, cells were detached incubating them with trypsin-EDTA 1% (GIBCO Life Technology, USA) at 37°C for 5' and re-plated respectively in a 25 $cm^2$ or 75 $cm^2$ flask.

**Fig. 18.** Flow chart of the experimental procedure for the Hy-Tissue SVF® study.

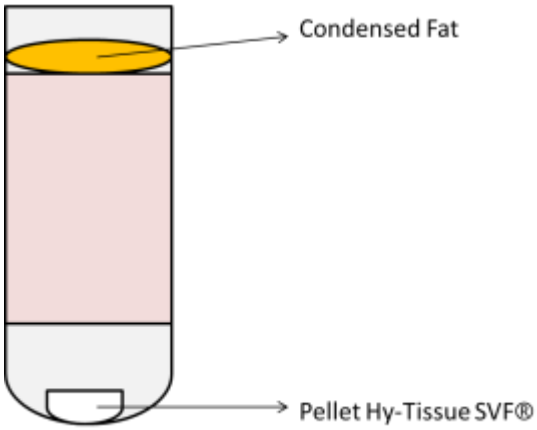


**Fig. 19.** Hy-Tissue SVF® product after centrifugation.

#### 4.1.7.3.2.3. Morphological analysis and cell viability test

At confluence, the cells were observed under a light microscope (Optika Microscopes Italy) furnished with a Leica camera at 20x magnification. Pictures of cells obtained with the three different Rigenera® operating timings, enzymatic method and from the two different harvesting sites were taken.

Cell viability and growth rate were evaluated by the cell viability test with trypan blue exclusion method. Cell suspension and trypan blue were mixed 1:1. The solution was put in a Bürker chamber and cells were counted under a light microscope at 20x magnification, excluding the blue non-viable cells. The growth rate was determined by the growth curve.

#### 4.1.7.3.2.4. CFU-F assay

3000 cells from each treatment were seeded in triplicate in 6-well plates and after 7 days of culture the adherent cell colonies were counted.

#### 4.1.7.3.2.5. Immunophenotyping

At confluence, the cells were detached with trypsin-EDTA. Around 200000 cells were placed in each Eppendorf tube. The pellet was washed with 1 mL of 1% FBS in PBS. 5 µl of the dead cell dye propidium iodide (PI) were added to one sample and it was incubated for 10'. The other samples were labelled with fluorescent-dye conjugated antibodies in a final volume of 100 µL of 1% FBS in PBS and incubated for 30' in ice. The herein examined antibodies were: PerCP-Cyt5.5-conjugated CD105 (dilution 1:20), BV421-conjugated CD73 (dilution 1:20), PE-conjugated CD34 (dilution1:5). All the antibodies were purchased from BD Biosciences, Becton Dickinson Italy S.p.A., Milan. After the incubation, the pellet was rinsed, resuspended in 300 µL of 1% FBS in PBS and transferred in flow cytometry tubes. The immunophenotyping was performed through a FACS canto II (BD, Becton Dickinson, Italy).

#### 4.1.7.3.2.6. Scanning electron microscopy (SEM)

Specimens of lipoaspirates and Hy-Tissue SVF® product were fixed with glutaraldehyde 2% in 0.1 M PB, post-fixed in 1% osmium tetraoxide ($OsO_4$) in the same buffer for 1h, dehydrated in concentrations of acetone, critical point dried (CPD 030, Balzers, Vaduz, Liechtenstein), fixed to stubs with colloidal silver, sputtered with gold by an MED 010 coater (Balzers), and examined with a FEI XL30 scanning electron microscope (FEI Company, Eindhoven, Netherlands).

#### 4.1.7.3.3. Results

After three days of culture, the attached cells from Hy-Tissue SVF® treatment appeared to have a morphology similar to the control, represented by the collagenase digestion. Indeed, their shape was long and thin, with a large and round nucleus. However, their number was much lower. Furthermore, it was possible to observe that more cells grew in the flask of post-massage compared to the one of Klein discard solution (fig. 20).

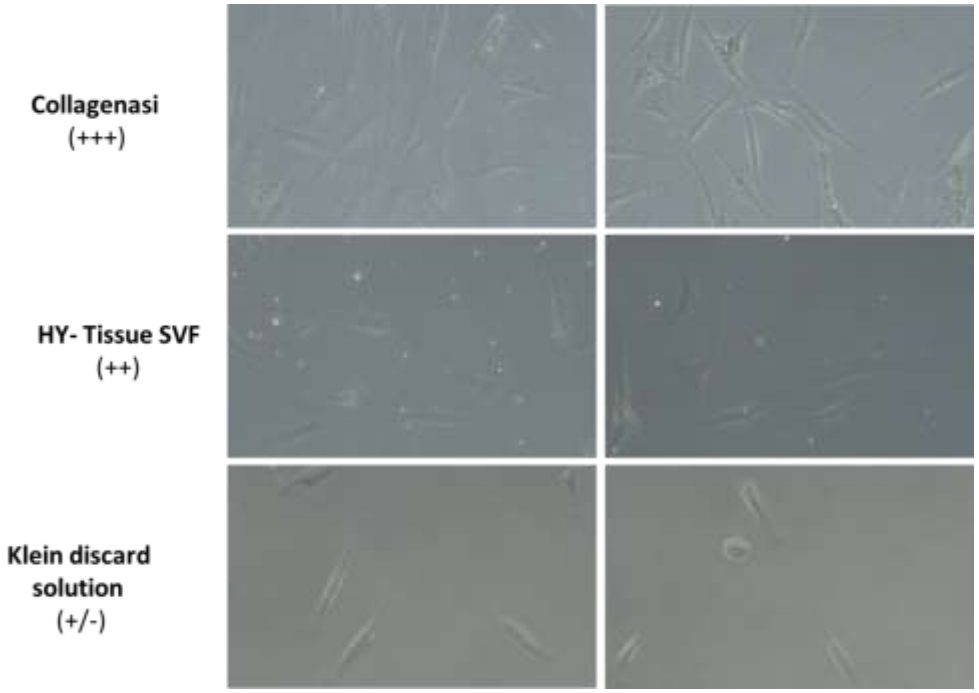


**Fig. 20.** Microscopic images (10x) of ASCs from collagenase (line 1), Hy-Tissue SVF® post-massage (line 2) and Hy-Tissue SVF® Klein discard solution (line 3). The cell morphology looked similar for all the flasks, but the number of attached cells was lower in the last one.

The first count was performed immediately after isolation and refers to both ASCs and the other cells belonging to the SVF. On average, the Hy-Tissue SVF® (post-

massage) yield resulted to be 25% compared to collagenase, the Klein discard solution yield resulted to be 8% of collagenase (fig. 21).

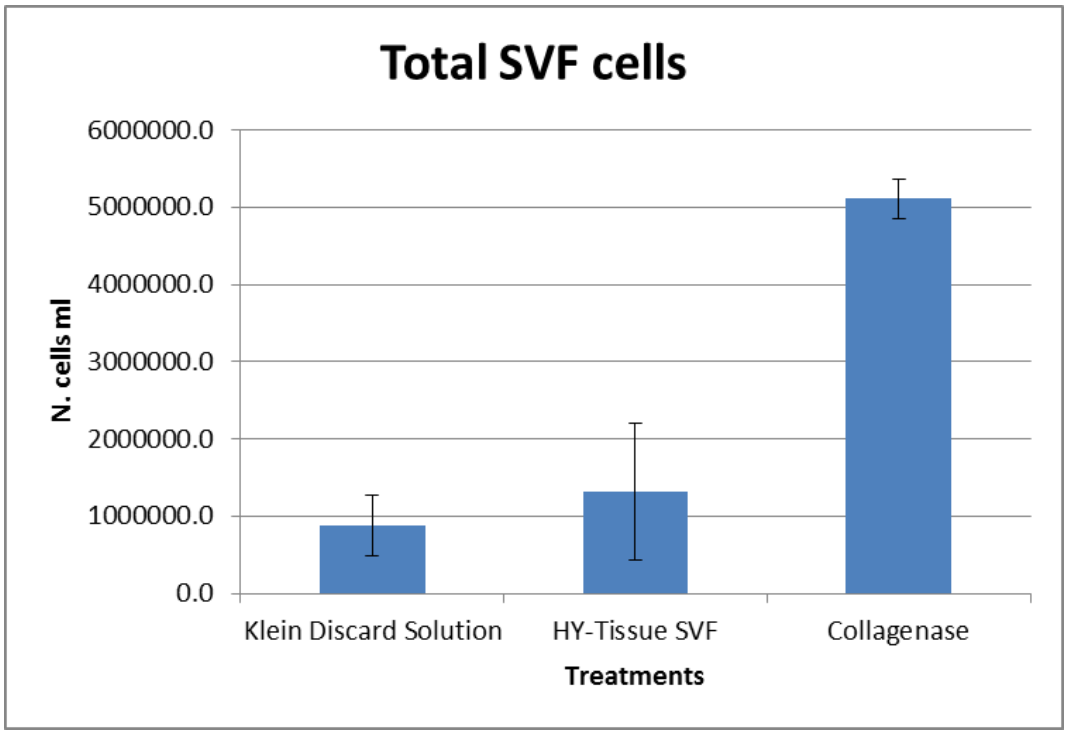


**Fig. 21.** SVF cells count after isolation. Hy-Tissue SVF® cells were around 25% of collagenase digestion cells and Klein discard solution cells were about 8% of cells from collagenase digestion.

Once the isolated cells were put in culture, only ASCs attached to the plastic flasks and therefore, were selected. ASCs from collagenase digestion reached the confluence (around 11000 cells) in 5 days, whereas the Hy-Tissue SVF® cells in almost the double of the time. Finally, the growth of ASCs from Klein waste solution was extremely slow and they did never reached the confluence and were discarded after 18 days, when the growth had almost stopped (fig. 22).

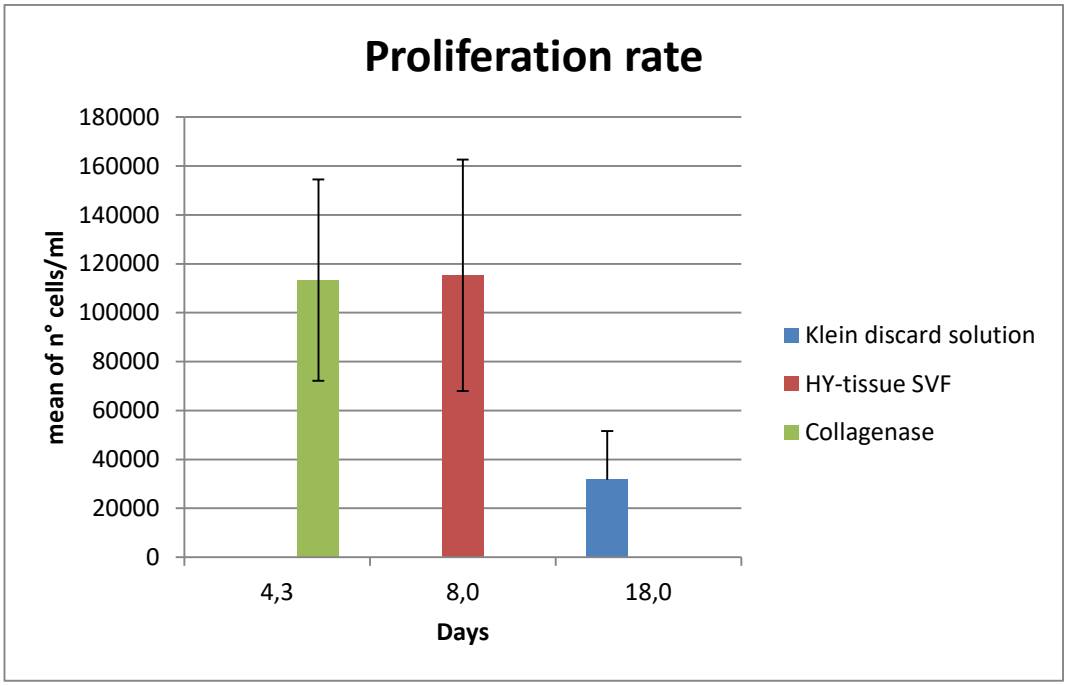


**Fig. 22.** Proliferation rate of cells from collagenase digestion, Hy-Tissue SVF® processing and Klein discard solution. The first ones grew slightly faster than the second ones. The last ones grew extremely slowly and were discarded.

The number of CFU after 7 days from cells seeding was more than three times higher with the collagenase digestion than with the post-massage and six times higher than with the pre-massage (fig. 23).

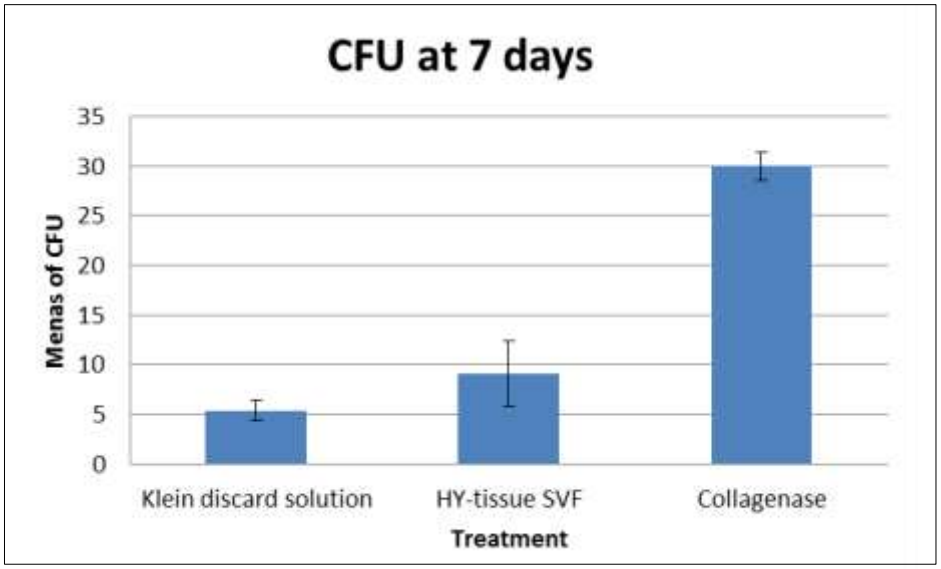


**Fig. 23.** CFU counting after 7 days. CFU after collagenase were much more than after Hy-Tissue SVF® processing.

At passage 0, the immunophenotypic analysis of Hy-Tissue SVF® cells after marking cells with propidium iodide (PI), a mortality marker, revealed that the percentage of alive cells was closed to 100% (fig. 24).

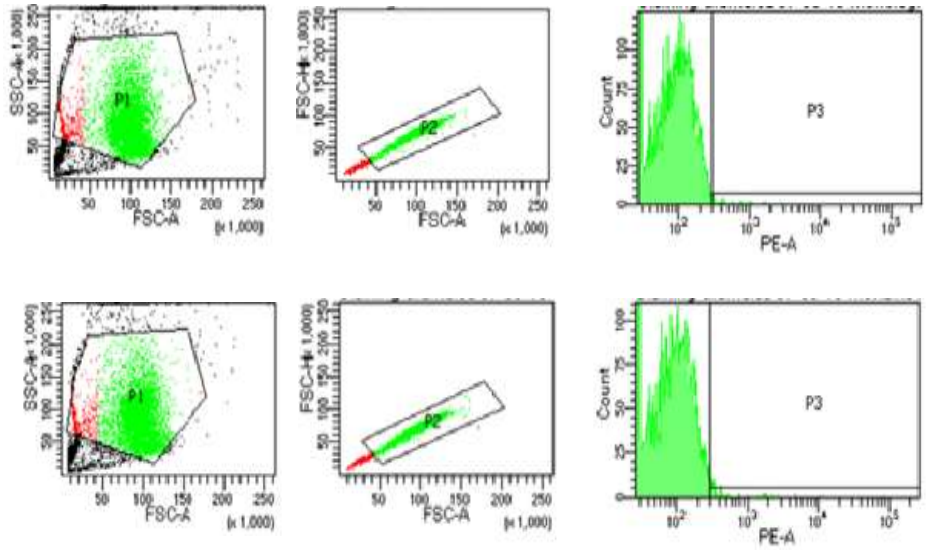


**Fig. 24.** Cell viability test at passage 0. Cells after Hy-Tissue SVF® processing resulted to be alive.

At passage 0, the percentage of positive cells for both the mesenchymal markers CD105 and CD73 and the haematopoietic marker CD34 was 2,1% for Hy-Tissue SVF® and 5,9% for collagenase digestion (the data evidencing the different percentages are not shown). The control, represented by the no marked cells, were all negative for these antibodies (fig.25).

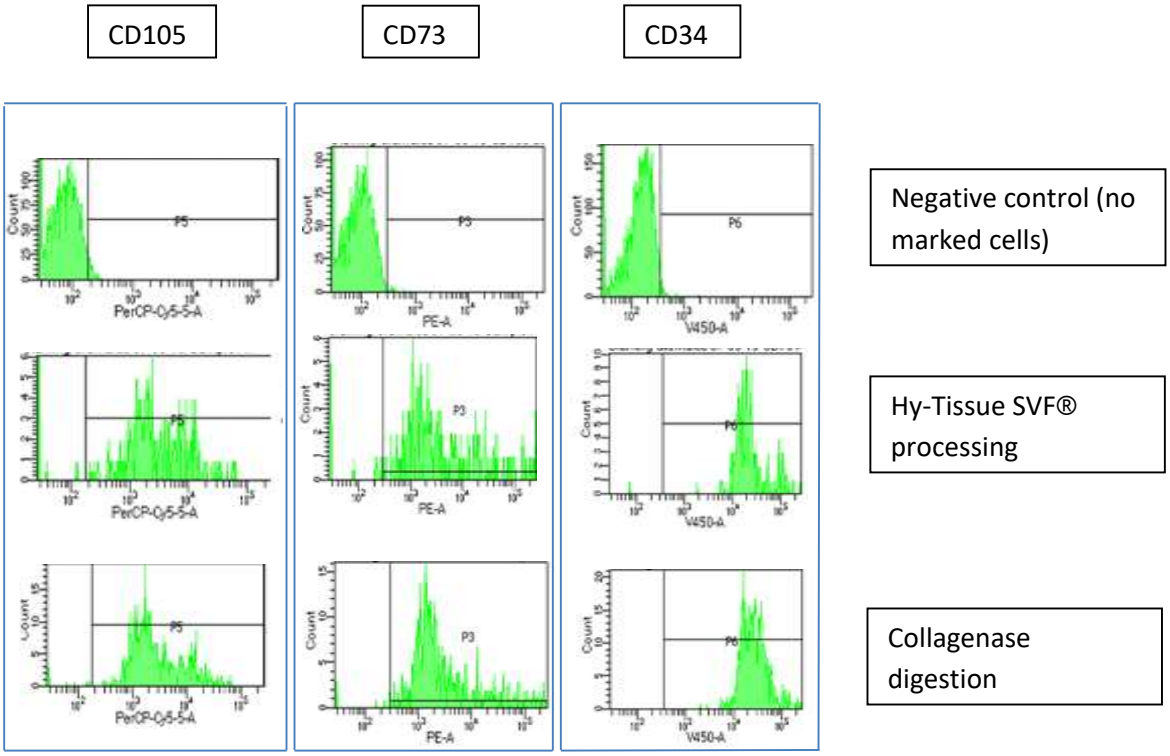


**Fig. 25.** Immunophenotyping at passage 0 of negative control, Hy-Tissue SVF® processing and collagenase digestion.

The immunophenotyping was also performed at higher passages of culture (p=10) and cells resulted to be positive for the mesenchymal markers (CD105 and CD73) and negative for the hematopoietic one (CD34) (data not shown).

Optical microscopy and SEM of lipoaspirates, before processing, revealed the presence of adipocytes aggregates having a diameter ranging from 1 to 2 mm.

Instead, the diameter of condensed fat aggregates, obtained after Hy-Tissue SVF® processing, was smaller (around 500 µm) (fig. 26).

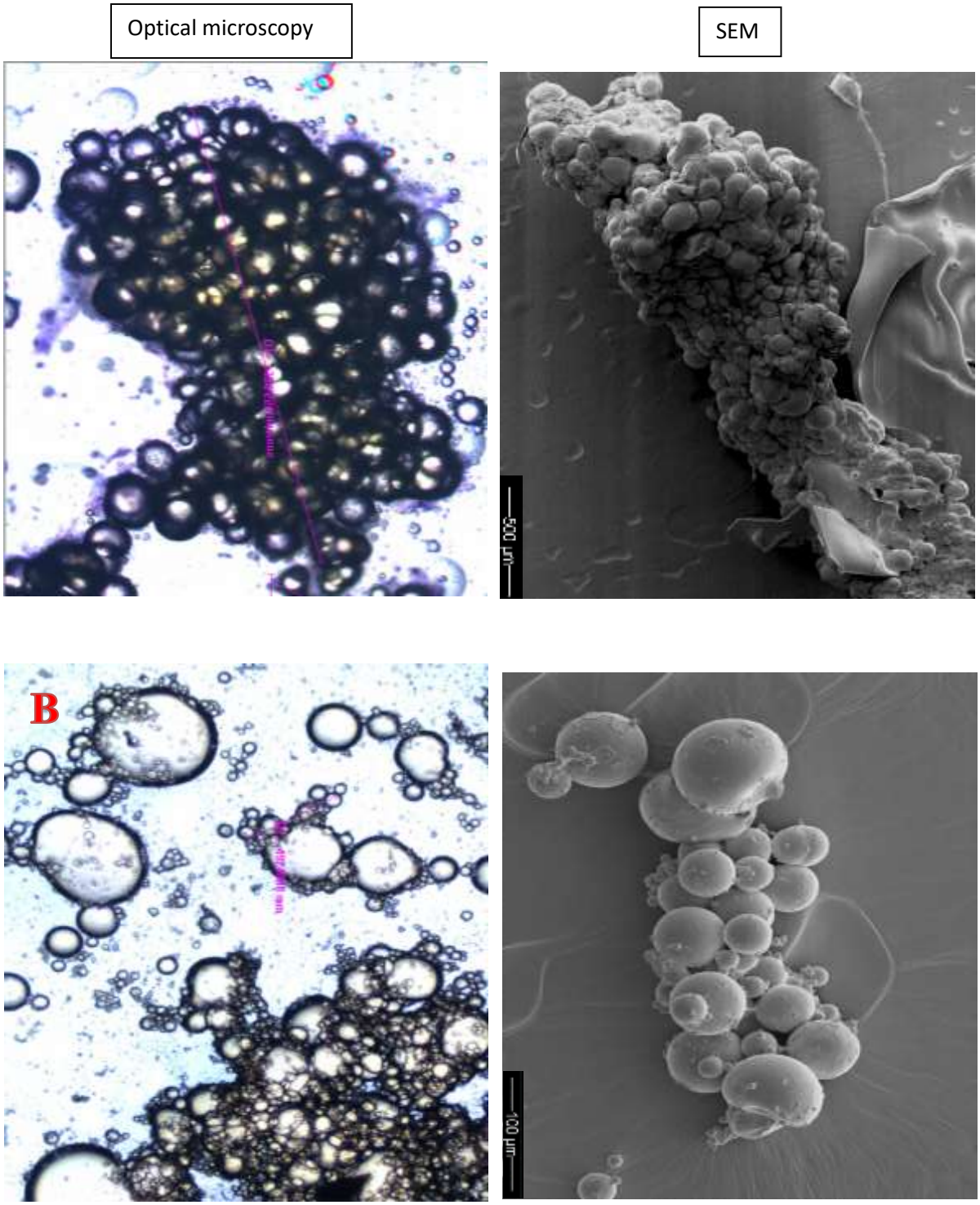


**Fig. 26.** Optical microscopy and SEM of adipocytes aggregates before (A) and after processing (B).

#### 4.1.7.3.4. Discussion

Hy-Tissue SVF® was invented to undergo the European restriction concerning the clinical use of enzymatic methods to process adipose tissue. Therefore, the two techniques have been compared *in vitro* in the present study. The cell morphology, viability and phenotype were not affected by the Hy-Tissue SVF® technique. Unfortunately, the cell yield and the replication rate resulted much lower than with collagenase digestion. Optical microscopy and SEM demonstrated that the processing was able to produce micrografts with diameter of around 500 µm constituted by aggregates of adipocytes. Instead, in the Klein discard solution only a small number of cells was present. A limitation of Hy-Tissue SVF® technique was that the entire procedure needed to be performed manually, so it was too much dependent on the operator, with a consequent large variability among the samples.

#### 4.1.7.3.5. Conclusion

Hy-Tissue SVF® technique could have been a valid clinical alternative to collagenase digestion, if the procedure had been completely automatized.

Anyway, further work needs to be performed to validate the method. First, some molecular analysis should be executed to determine the expression level of genes involved, for instance, in stemness, adipogenic, osteogenic and chondrogenic differentiation, angiogenesis, inflammation and cell aging. Secondly, the experiments should be translated *in vivo* in an animal model in order to reproduce the biological pathways occurring in the human species.

#### *4.1.7.4. Hy-tissue Nanofat® (Fidia Farmaceutici, Abano Terme, Padua, Italy)*

##### 4.1.7.4.1. Introduction

Hy-tissue Nanofat® is a disposable kit constituted by a 10 mL collection bag with a 120 μm filter and a Teflon insert, three 10 mL removable plunger syringes and syringe caps. Two syringes are screwed to the bag and the lipoaspirate is injected inside. The fat is mechanically emulsified shifting it 30 times between the two syringes. Afterwards, the emulsion is transferred to the bag. The final product is aspired by another 10 mL syringe from the bottom of the collection bag [74], [75].

The general aim of the present study was to deeply analyze the efficacy of the Hy-tissue Nanofat® procedure *in vitro* and the results were compared with the gold-standard collagenase digestion.

**Fig. 27.** Hy-Tissue Nanofat® device [75].

#### 4.1.7.4.2. Material and methods

##### 4.1.7.4.2.1. Adipose tissue samples collection

Adipose tissue was harvested by 5 women subjected to liposuction, aging between 48 and 55 years old. Patients signed the informed consents before the tissue collection. The water-assisted liposuction named BEAULI® protocol was used. It is described in detail in [72].

##### 4.1.7.4.2.2. Cell isolation and culture

Each adipose tissue sample (15 mL) was divided in 2 portions. 5 mL of lipoaspirate were digested with collagenase following the collagenase protocol, as reported in [23]. The remaining 10 mL were processed with the Hy-Tissue Nanofat® device. All the samples were centrifuged at 3000 rpm for 7'. Afterwards, they were incubated with 10 mL of Red Blood Cell Lysis Solution (Miltenyi Biotec, Germany) for 10' at room temperature, to lyse the erythrocytes. For the Fibloblastic-Colony-Forming Unit (CFU-F) assay, 3000 cells were resuspended in 2 mL of complete medium, plated in a 6-well plate (BD FalconTM, Becton Dickinson, Italy) and incubated at 37°C and 5% $CO_2$. Other 10000 cells were resuspended in 6 mL of complete medium, plated in a 25 $cm^2$ flask (BD FalconTM, Becton Dickinson, Italy) and incubated at 37°C and 5% $CO_2$. The media were first changed after 72 hours and, successively, every 24 hours. At confluence, cells were detached incubating them with trypsin-EDTA 1% (GIBCO Life Technology, USA) at 37°C for 5' and re-plated respectively in a 25 $cm^2$ or 75 $cm^2$ flask.

#### 4.1.7.4.2.3. Morphological analysis and cell viability test

At confluence, the cells were observed under a light microscope (Optika Microscopes Italy) furnished with a Leica camera at 20x magnification.

Cell viability and growth rate were evaluated by the cell viability test with trypan blue exclusion method. Cell suspension and trypan blue were mixed 1:1. The solution was put in a Bürker chamber and cells were counted under a light microscope at 20x magnification, excluding the blue non-viable cells. The growth rate was determined by the growth curve.

#### 4.1.7.4.2.4. CFU-F assay

3000 cells from each treatment were seeded in triplicate in 6-well plates and after 7 days of culture the adherent cell colonies were counted.

#### 4.1.7.4.2.5. Immunophenotyping

At confluence, the cells were detached with trypsin-EDTA. Around 200000 cells were placed in each Eppendorf tube. The pellet was washed with 1 mL of 1% FBS in PBS and then labelled with fluorescent-dye conjugated antibodies in a final volume of 100 µL of 1% FBS in PBS and incubated for 30' in ice. The herein examined antibodies were: PerCP-Cyt5.5-conjugated CD105 (dilution 1:20), BV421-conjugated CD73 (dilution 1:20), PE-conjugated CD34 (dilution1:5), BV650-conjugated CD45 (dilution 1:20). All the antibodies were purchased from BD Biosciences, Becton Dickinson Italy S.p.A., Milan. Alexa Fluor-488-conjugated SEEA3 (dilution 1:20) was purchased from Aurogene S.R.L, Rome. After the incubation, the pellet was rinsed, resuspended in 300 µL of 1% FBS in PBS and transferred in flow cytometry tubes. The immunophenotyping was performed through a FACS canto II (BD, Becton Dickinson, Italy).

#### 4.1.7.4.3. Results

Images at optical microscope showed that cells from Hy-Tissue SVF® had the typical morphology of ASCs (fig. 28).

**Fig. 28.** Image of ASCs obtained from Hy-Tissue SVF® processing technique.

The first count was performed immediately after isolation and refers to both ASCs and the other cells belonging to the SVF. On average, the Hy-Tissue SVF® (post-massage) yield resulted to be 10% compared to collagenase (fig. 29).

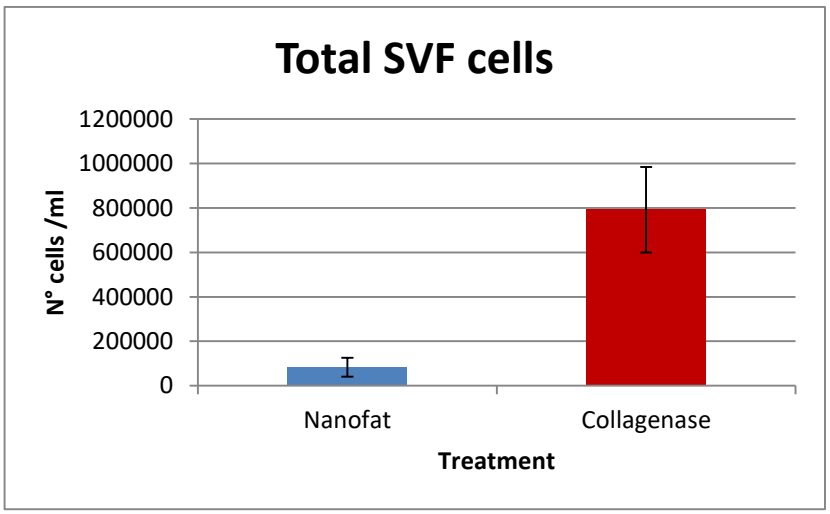


**Fig. 29.** SVF cells count after isolation. Hy-Tissue SVF® cells were around 10% of collagenase digestion cells.

Once the isolated cells were put in culture, only ASCs attached to the plastic flasks and therefore, were selected. The proliferation rate of ASCs from Hy-Tissue Nanofat® was about half of those from collagenase digestion. (fig. 30).

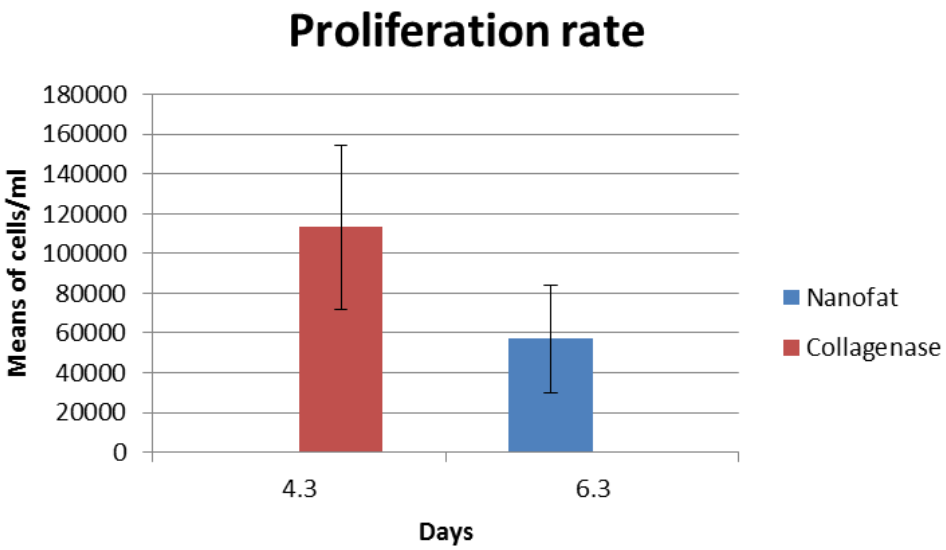


**Fig. 30.** Proliferation rate of cells from collagenase digestion and Hy-Tissue Nanofat® processing. The first one was the was around the double of the second one.

The number of CFU after 7 days from cells seeding for Hy-Tissue Nanofat® was the 69% of the number of CFU for collagenase digestion (fig. 31).

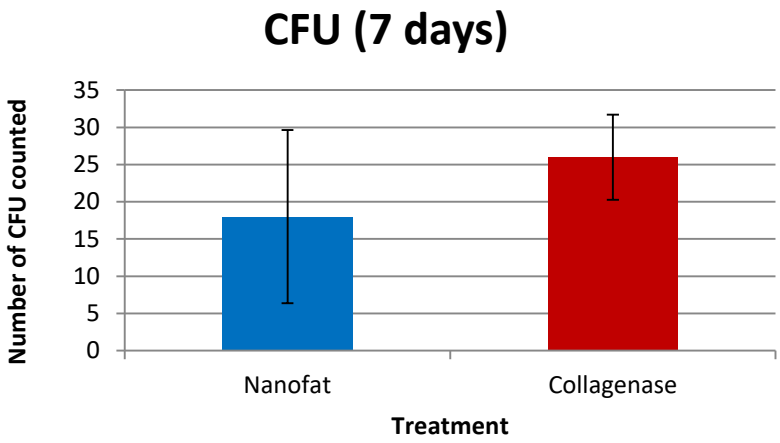


**Fig. 31.** CFU counting after 7 days. CFU after Hy-Tissue SVF® processing were the 69% of CFU after collagenase digestion.

At passage 0, the percentage of positive cells for both the mesenchymal markers CD105 and CD73 and the haematopoietic marker CD34 was 2,7% for Hy-Tissue SVF® (the data evidencing the percentage are not shown) (fig.32).

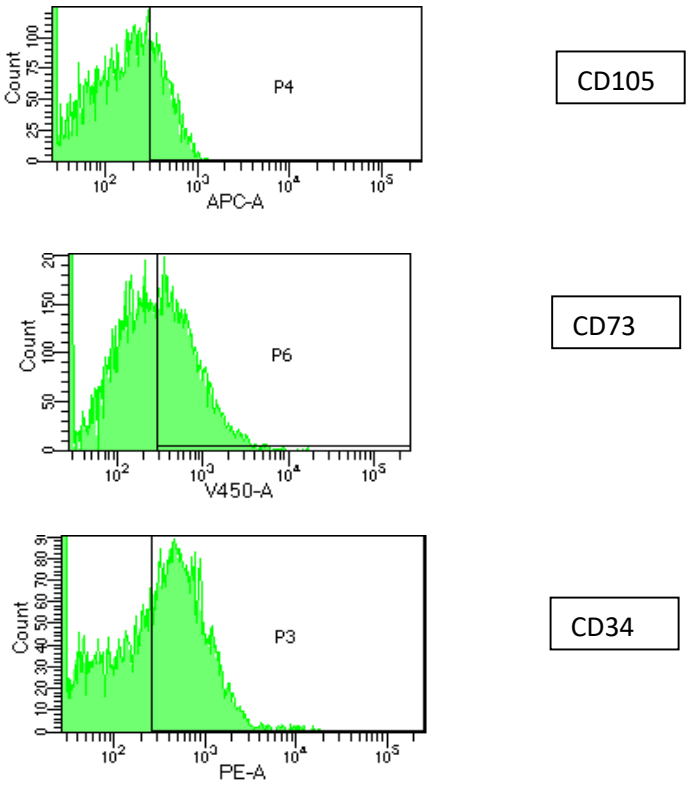


**Fig. 31.** Immunophenotyping at passage 0 of Hy-Tissue SVF® processing.

At higher passages (p2 and p10), the mesenchymal markers (CD105 and CD73) were highly expressed, whereas the hematopoietic markers were almost no expressed (CD45 and CD34). The expression of SSEA3 antigen, identifying the MUSE population, was quite variable (fig. 32).

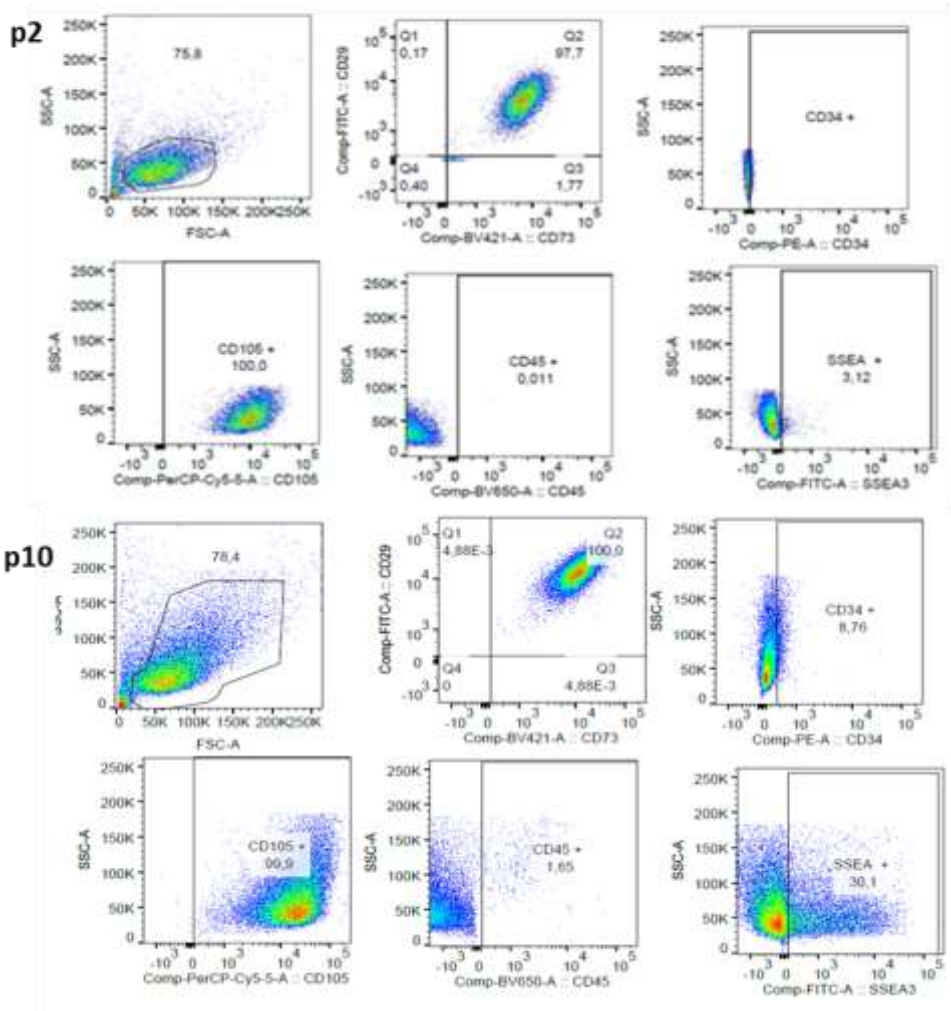


**Fig. 32.** Immunophenotyping of ASCs derived from Hy-Tissue Nanofat® at passages 2 and 10.

#### 4.1.7.4.4. Discussion

Hy-Tissue Nanofat® was invented to undergo the European restriction concerning the clinical use of enzymatic methods to process adipose tissue. Therefore, the two techniques have been compared *in vitro* in the present study. The cell morphology, viability and phenotype were not affected by the Hy-Tissue Nanofat® technique, also over time at higher passages. Unfortunately, the cell yield and the replication rate resulted much lower than with collagenase digestion. As the previously analysed Hy-Tissue SVF®, a limitation of the present technique was that the entire procedure needed to be performed manually, so it was too much dependent on the operator, with a consequent large variability among the samples.

#### 4.1.7.4.5. Conclusion

Hy-Tissue Nanofat® technique could have been a valid clinical alternative to collagenase digestion, if the procedure had been completely automatized.

Anyway, further work needs to be performed to validate the method. First, some molecular analysis should be executed to determine the expression level of genes involved, for instance, in stemness, adipogenic, osteogenic and chondrogenic differentiation, angiogenesis, inflammation and cell aging. Secondly, the experiments should be translated *in vivo* in an animal model in order to reproduce the biological pathways occurring in the human species.

#### *4.1.7.4. General conclusion*

Rigenera®, Hy-Tissue SVF® and Hy-Tissue Nanofat® are three different techniques to process adipose tissue after liposuction and before injection for autologous fat transfer. They are all able to isolate SVF and ASCs but with different yields, comparing them with the respective yield of collagenase digestion, which was considered 100%. Indeed, the SVF isolation yield of Hy-Tissue SVF® was around 25%, whereas the one of the other two procedures about 10%. Also, the cell replication rate for Hy-Tissue SVF® was around 60%, for Hy-Tissue Nanofat® about 45% and for Rigenera® about 40%. However, the standard deviation was much smaller, and thus the reproducibility was much higher with Rigenera® since it is automated and, therefore independent of the operator.

## *4.2. Adipose tissue engineering*

### 4.2.1. Introduction

#### *4.2.1.1. What is tissue engineering?*

Tissue engineering is the use of living cells, biocompatible materials and biochemical or physical factors to create human tissues, with the aim to replace the injured or damage original ones. It is considered a promising solution to overcome the present shortage of organ donor and the long transplant waiting list. In tissue engineering, different structures can be used: only cells, only scaffolds or a combination of both. Scaffolds can be classified in: autografts, which are built from the patient's cells, allografts, deriving from another individual and xenografts, coming from animals. They can also be divided in natural (i.e. collagen, hyaluronic acid, chitosan, alginate), which derive from natural extracellular materials and synthetic (i.e. polycaprolactone (PCL), polylactic acid (PLA), polyglycolic acid (PGA)), which are built with artificial material, but miming the natural ones. Optimal scaffolds should have specific characteristics: promoting cell adhesion and proliferation, biocompatibility, biodegradability, mechanical integrity and porosity, adhesion motifs. Scaffolds can have a conductive role, when they simply fill the empty spaces, inductive role, when they deliver bioactive molecules and supportive role, when they deliver cells [76], [77].

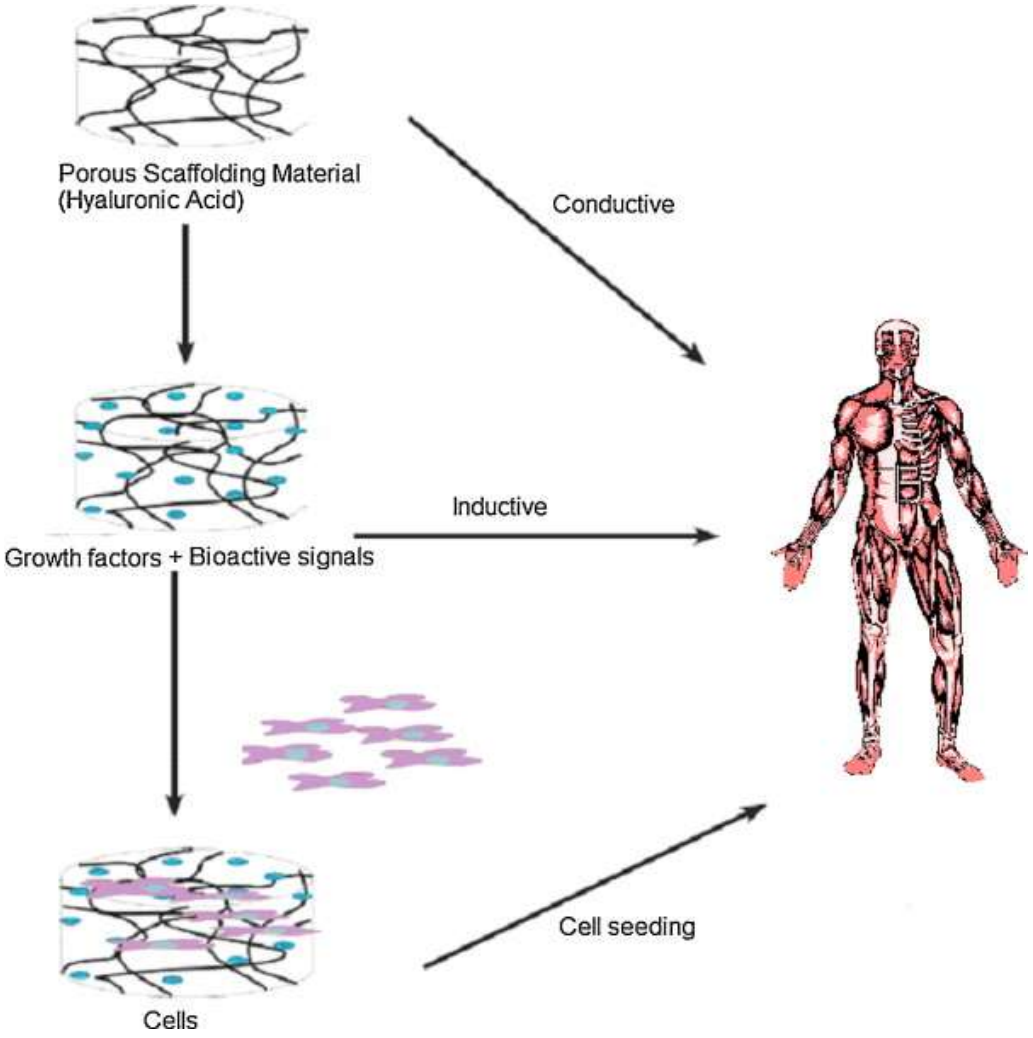


**Fig. 33.** Supportive, conductive and inductive roles of scaffolds [77].

A further scaffold classification can be made on the basis of fabrication methods: hydrogels, which are 3D networks of polymers that absorb a large amount of water, fiber and nano-fiber scaffolds, which are made by electrospinning, 3D printed scaffolds, which are made by bioprinters and leached scaffolds, whose fabrication is template-guided [78], [79].

#### *4.2.1.2. Hyaluronic acid*

Hyaluronic acid (HA) is a linear polysaccharide constituted of repeating disaccharide units of D-glucuronic acid and N-acetyl-D-glucosamine linked by β-1-4.

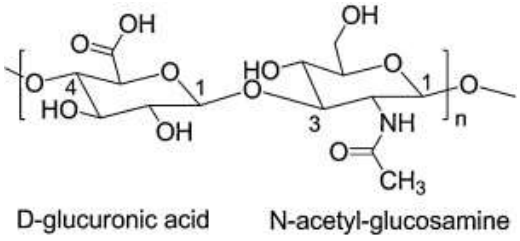


**Fig. 34.** Chemical structure of hyaluronic acid [80].

It is the primary component of the extracellular matrix of the connective tissue. It is also abundant in the skin, in the synovial joint fluids, in hyaline cartilage and intervertebral disc nucleus.

It plays important roles in the body, such as lubrication of arthritis joints and in some cell functions, such as cell motility and cell matrix adhesion. In human organisms, it is synthetized by membrane-bound synthases, can be obtained by enzymatic digestion from different tissue and is also produced by bacteria.

Thanks to its biocompatibility, biodegradability, versatility and its unique chemical-physical properties, such as the high viscoelasticity, it finds many applications in different fields of medicine. For instance, it can be used as a marker for certain cancers and liver diseases. Moreover, it can be injected in joints in case of osteoarthritis, reducing the inflammation and promoting the synthesis of cartilage and endogenous hyaluronic acid. In addition, it is used to lubricate and reduce irritation of eyes, being a component of artificial tears. Moreover, it is the most common cosmetic filler, since it elasticizes the skin and corrects esthetic defects. Finally, it is often used as a drug delivery polymer, improving the drug cellular uptake and efficacy.

#### *4.2.1.3. Hyaluronic acid hydrogels for tissue engineering*

In order to form a hydrogel, hyaluronic acid needs to be chemically modified. Esterification or crosslinking of carboxyl or hydroxyl group with other molecules, such as glutaraldehyde, represent the most used strategies to obtain it. Crosslinking strategies are also used to control the HA degradation rate, which naturally occurs in physiological environments through hyaluronidases. Small and medium chain

lengths of hyaluronic acid have pro-angiogenic and anti-apoptotic properties. [81] HA-based hydrogels have many applications in tissue engineering, among them cartilage repair, wound healing and skin regeneration, retinal regeneration, cardiovascular tissue engineering, brain and neural regeneration and lung regeneration. [77], [82].

#### *4.2.1.4. Mechanism of cell behavior regulation by hyaluronic acid*

Hyaluronic acid directly interacts with many stromal cell surface receptors and activate some intracellular signals, influencing important cell functions, such as survival, motility or differentiation. The main receptor is Cluster determinant 44 (CD44). Thanks to this association, an intracellular signal cascade is activated in response to extracellular matrix signals. CD44 is also involved in the maintenance of cartilage homeostasis and in the catabolism of hyaluronic acid. In addition, HA regulates chemokines, metalloproteinases and tissue inhibitors, which are essential for the building of an efficient scaffold.

#### *4.2.1.5. Application of HA-based scaffold pre-seeded with MSCs in regenerative medicine*

As amply described in the review [83], hyaluronic acid scaffolds, alone or in combination with other materials, can interact with MSCs and promote, both *in vitro* and *in vivo*, chondrogenesis, osteogenesis, adipogenesis, wound healing, regeneration of ligaments and tendons, muscles and also induce MSCs differentiation into insulin-producing cells, hepatocyte-like cells, neurons and glial cells.

### 4.2.2. *In vitro* interaction among hyaluronic acid and ASCs

#### *4.2.2.1. Introduction*

Scientific literature amply described the ability of hyaluronic acid to promote the differentiation of MSCs into different mature cell types, as summarized in [83]. However, very few researches focused on adipogenesis.

The present study aims to investigate the interaction among hyaluronic acid and ASCs. Specifically, this first part shows some *in vitro* experiments, which had the following objectives:

1. To test the cytotoxicity of three hyaluronic acid powders and three hydrogels all crosslinked and having different molecular weights and their ability to promote the adipogenesis of ASCs;

2. to test the interaction between one hyaluronic acid sponge and ASCs.

#### *4.2.2.2. Material and methods*

##### 4.2.2.2.1. Hyaluronic acid formulations

Hyaluronic acid powders (50 kDa, 200 kDa and 1000 kDa), crosslinked hydrogels (Hyal-System, Hyal-ACP and Hyal-DUO) and FID-119 sponge (200 kDa), provided by Fidia Framaceutici SpA (Abano Terme, Padua, Italy) were tested in this in vitro study.

##### 4.2.2.2.2. Adipose tissue samples collection

Adipose tissue was harvested by 10 women subjected to liposuction, aging between 43 and 61 years old. Patients signed the informed consents before the tissue

collection. The water-assisted liposuction named BEAULI® protocol was used. It is described in detail in [72].

#### 4.2.2.2.3. Cell isolation and culture

5 mL of lipoaspirate were digested with collagenase following the collagenase protocol, as reported in [23]. Afterwards, they were centrifuged at 3000 rpm for 7'. Then, they were incubated with 10 mL of Red Blood Cell Lysis Solution (Miltenyi Biotec, Germany) for 10' at room temperature, to lyse the erythrocytes. Cells were resuspended in 6 mL of complete medium, plated in a 25 $cm^2$ flask (BD FalconTM, Becton Dickinson, Italy) and incubated at 37°C and 5% $CO_2$. The medium was first changed after 72 hours and, successively, every 24 hours. At confluence, cells were detached incubating them with trypsin-EDTA 1% (GIBCO Life Technology, USA) at 37°C for 5' and re-plated respectively in a 25 $cm^2$ or 75 $cm^2$ flask.

#### 4.2.2.2.4. Powders and fillers: citotoxicity assay

To evaluate the cytotoxicity, 1000 ADAS were seeded in 24-well plates with DMEM+10%FBS+1%P/S. After 24 hours, the following HA concentration were administered in duplicate in the wells: 20 mg/ml medium, 10 mg/ml medium, 2 mg/ml medium, 1 mg/ml medium, 500 µg/ml medium, 100 µg/ml medium, 2 µg/ml medium. After 3, 7 and 14 days, ADAS were detached with trypsin-EDTA 1% for 5' at 37°C, centrifuged for 5' a 400 g and resuspended in sterile PBS. As a negative control, one sample was not treated, whereas, as a positive control, one sample was exposed to high temperature (59°C) for a long time (60'). 5 µl of the dead cell dye propidium iodide (PI) were added to all samples. The fluorescence was detected through the flow cytometer BD FACS Canto II (BD Bioscience).

#### 4.2.2.2.5. Powders and fillers: adipogenesis evaluation

To evaluate the adipogenesis, ADAS were seeded on glasses placed on the bottom of wells in 24-well plates with DMEM+10%FBS+1%P/S. After 24 hours, they were incubated with hyaluronic acid at 37°C for 3, 7 and 14 days. At every time-point, cells were fixed with a mix of glutaraldehyde 2% and paraformaldehyde 2% (1:1 v/v) for 1 hour at 4°C and then glasses were removed from the wells. Afterwards, ADAS were incubated with the antibody Alexa Fluor 647-coniugated anti-GLUT4 (Novus Bio), receptor of mature adipocytes, for 30' at 4°C. Successively, glasses were washed to remove the unspecific labelling, and were put on microscope slides and fixed with a mounting medium containing DAPI and an antifade solution. The cells were observed using the confocal microscope Leica Confocal, equipped with a CCD camera and images were elaborated using the software LASX.

#### 4.2.2.2.6. FID-119 sponge: transmission electron microscopy (TEM) of ASCs after incubation with FID-119

To evaluate the cell-scaffold interaction, ADAS were seeded on glasses placed on the bottom of wells in 6-well plates with DMEM+10%FBS+1%P/S and incubated at 37°C and 5% of $CO_2$. After 48 hours, medium was changed and two specimen of FID-119 (0.5 $cm^3$) were positioned in each well for 24 hours, 7 or 14 days. At each time point, the sponge and the medium were removed and ADAS were fixed with buffered formalin 10% for 1 hour. Afterwards, they were dehydrated in graded acetone, and impregnated with Epon 812 resin (Electron Microscopy Sciences, Hatfield, PA, USA). The glasses were placed on an aluminium foil and gelatin capsules were filled with the resin and turned upside-down onto the glasses. To induce resin polymerization, they were put in the oven at 60°C. Then, the resin blocks were detached from the glasses by dipping into liquid nitrogen for a few seconds. Ultrathin sections were cut with an UltraCut E ultramicrotome (Reichert-Jung, Leica Microsystems, Wetzlar, Germany) and observed using a Philips

Morgagni TEM (FEI Company Italia Srl, Milan, Italy), operating at 80 kV and equipped with a Megaview II camera for digital image acquisition.

#### 4.2.2.2.7. FID-119 sponge: scanning electron microscopy (SEM) of ASCs after incubation with FID-119

To evaluate the adipogenesis, ADAS were seeded on glasses placed on the bottom of wells in 6-well plates with DMEM+10%FBS+1%P/S and incubated at 37°C and 5% of $CO_2$. After 48 hours, medium was changed and two specimen of FID-119 (0.5 $cm^3$) were positioned in each well for 24 hours, 7 or 14 days. At the end of incubation times, specimens of sponges were fixed with glutaraldehyde 2% in 0.1 M PBS, post-fixed in 1% osmium tetraoxide ($OsO_4$) in the same buffer for 1h, dehydrated in concentrations of acetone, vacuum dried, fixed to stubs with colloidal silver, sputtered with gold by an MED 010 coater (Balzers), and examined with a FEI XL30 SEM (FEI Company, Eindhoven, Netherlands).

#### 4.2.2.2.8. FID-119 sponge: histological analysis

To evaluate the adipogenesis, ADAS were seeded on glasses placed on the bottom of wells in 6-well plates with DMEM+10%FBS+1%P/S and incubated at 37°C and 5% of $CO_2$. After 48 hours, medium was changed and two specimen of FID-119 (0.5 $cm^3$) were positioned in each well for 24 hours, 7 or 14 days. At each time point, after removal of the sponge and the medium, ADAS were washed with 0.1 M PBS and then fixed with 4% formalin in 0.05 M PBS for 20'. After washing with distilled water and 60% isopropanol for 2', cells were stained with a solution 0.35% of the lipid marker Oil Red O in isopropanol for 10' at room temperature. Then, they were washed with distilled water, stained with Mayer's Hematoxylin Bio-Optica solution for 1' at room temperature and washed again. Finally, Dako Faramount Aqueous Mounting Medium (Agilent) was added and the coverslip was applied. Samples were observed at light microscope Olympus BX-51, equipped with Nikon CCD camera and Image ProPlus 7.2 software.

### *4.2.2.3. Results*

#### 4.2.2.3.1. Powders and fillers

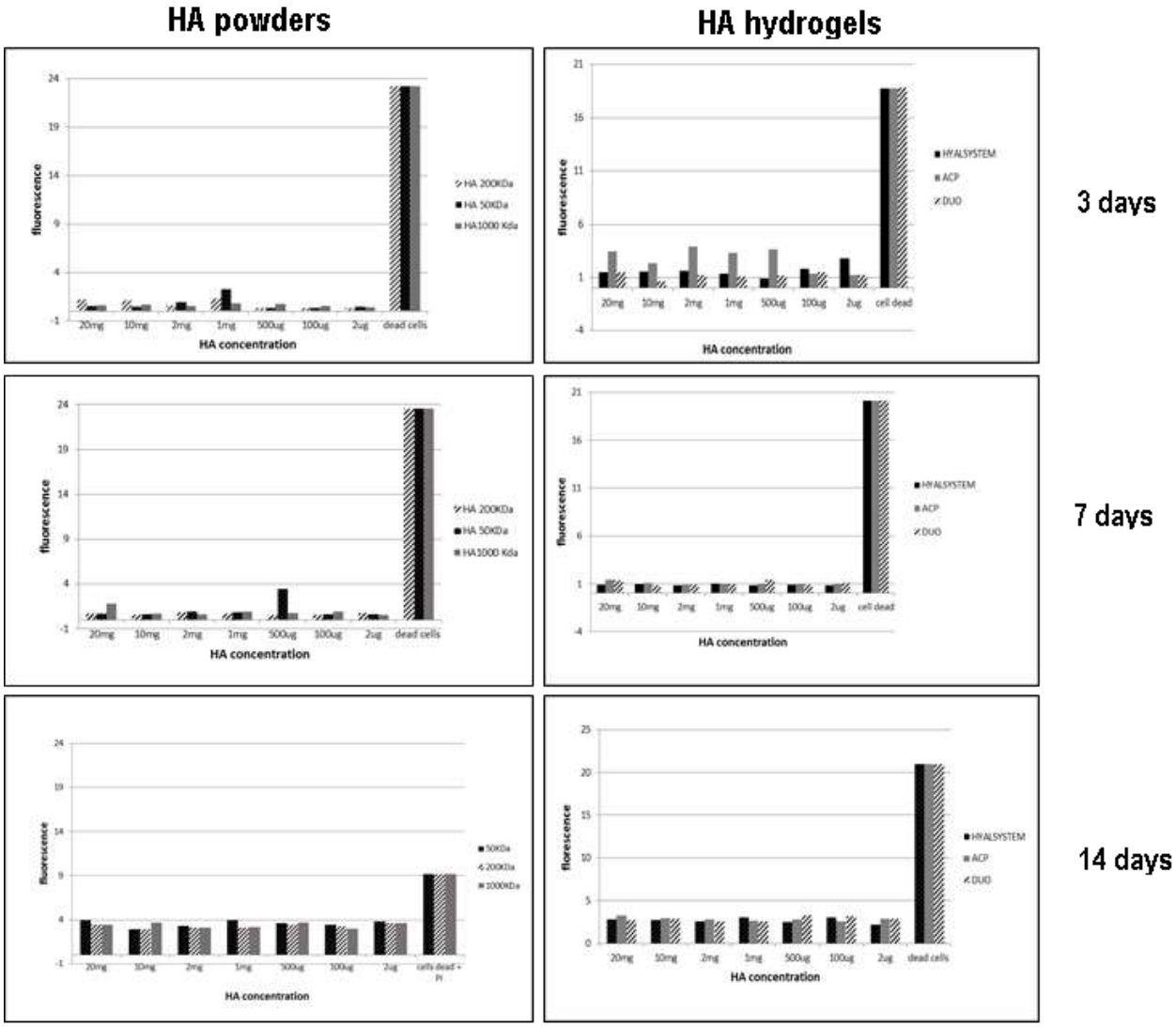


**Fig. 35.** Citotoxicity assay. HA powders (left panel) and hydrogels (right panel) cytotoxicity test. The cells were marked with PI (a fluorescent dye, which binds dead cells) and its fluorescence was measured by flow cytometry after 3, 7 and 14 days from HA incubation. Much lower fluorescence than positive controls (dead cells) was detected for each HA formulations and time point.

Fig. 35 shows the results of cytotoxicity analysis for HA powders (left panel) and hydrogels (right panel) at different time points (3, 7 and 14 days) from HA incubation. All these values were normalized, using negative controls, represented by non-treated normal-growing cells. For each condition, the respective positive control, represented by the maximum percentage of cell death, has been provided.

Obtained values of fluorescence of dead cells for powders were, on average, 10% of positive controls (100%) after 3 and 7 days and 50% of positive controls after 14 days (left panel). The fluorescence values of ASCs treated with hydrogels were around 10% of positive controls after 3 and 7 days of incubation and 15% of positive controls after 14 days (right panel).

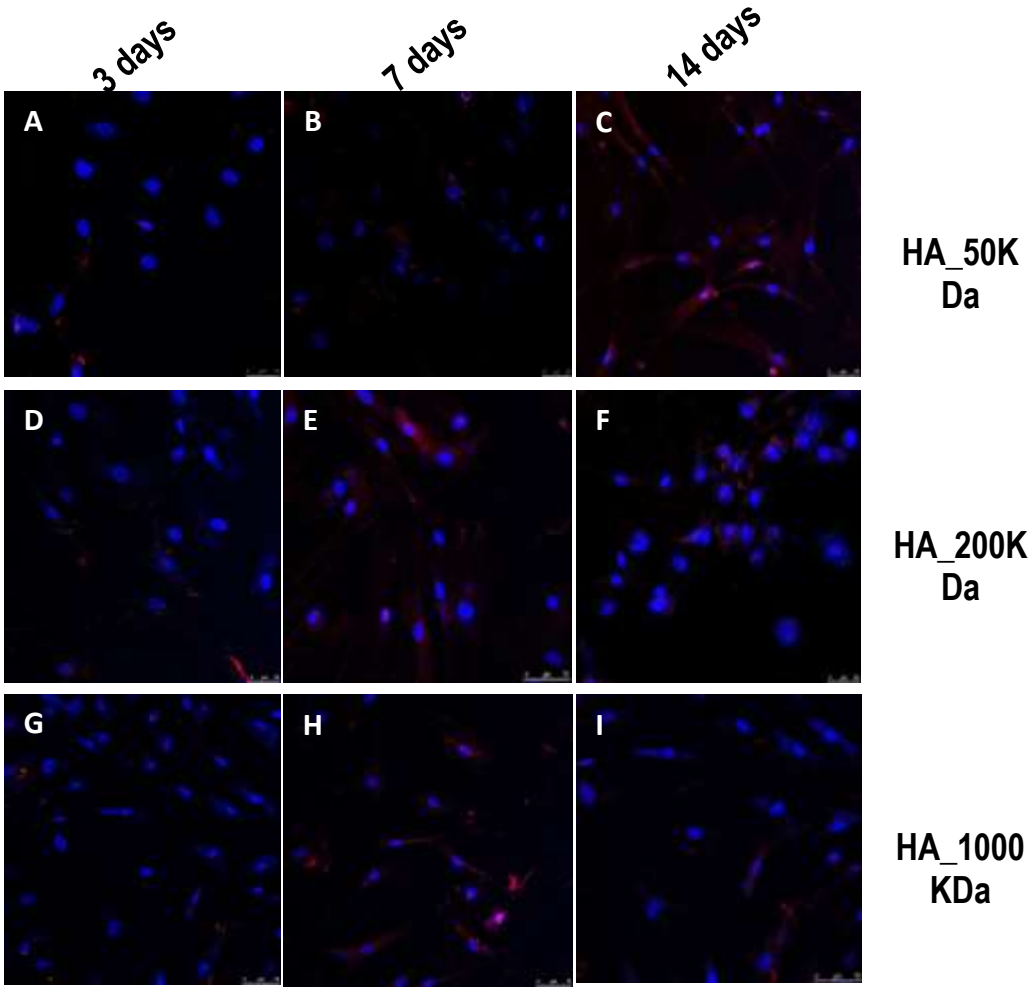


**Fig. 36.** Immunostaining of ASCs treated with HA powders. Cells labelled with anti-GLUT4 conjugated with Alexa Fluor 647 (red) and DAPI mounting medium (blue) were observed under confocal microscope after 3, 7 and 14 days from HA incubation. Images all refer to HA concentration equal to 20 mg/mL culture medium. A moderate red fluorescence was visible after 3 days of incubation (panels A, D, G), while higher fluorescence was visible after 7 (panels B, E, H) and 14 days of incubation (panels C, F, I).

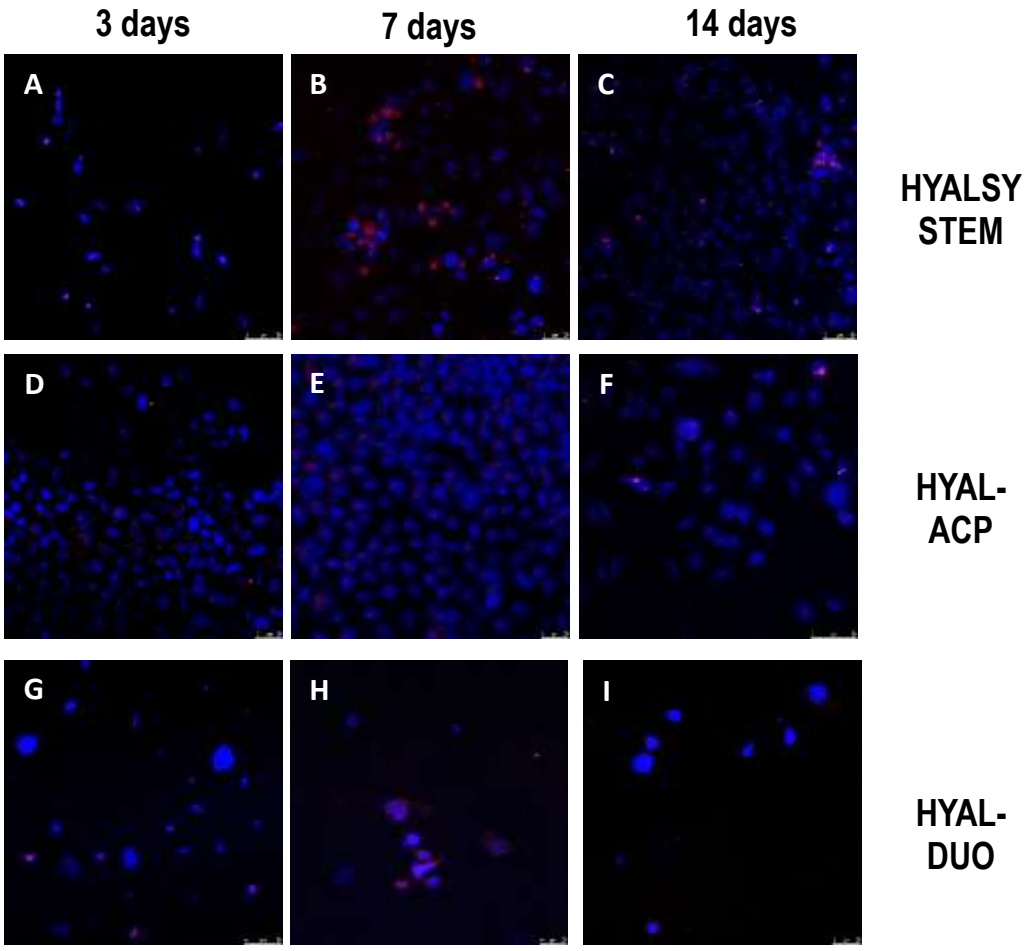


**Fig. 37.** Immunostaining of ASCs treated with HA hydrogels. Cells labelled with anti-GLUT4 conjugated with Alexa Fluor 647 (red) and DAPI mounting medium (blue) were observed under confocal microscope after 3, 7 and 14 days from HA incubation. Images all refer to HA concentration equal to 20 mg/mL culture medium. The highest level of fluorescence was visible after 3 and 7 days of incubation (panels A, D, G, B, E, H), while a less intense fluorescence was detectable after 14 days (panels C, F), being almost absent using Hyal-DUO hydrogel (panel I).

Fig. 36 and 37 show the results of the immunostaining of ASCs treated, respectively, with HA powders and hydrogels and labelled with anti-GLUT4 antibody, a receptor expressed in mature adipocytes, conjugated with the fluorophore Alexa Fluor 647 (red) and DAPI mounting medium (blue), which binds to cell nuclei. They were incubated with the different HA formulations for 3, 7 and 14 days and, afterwards, they were observed under confocal microscope.

ASCs incubated with 50 kDa, 200 kDa HA and 1000 kDa powders showed a level of red fluorescence, and therefore a GLUT4 level of expression, generally dependent on time. In fact, the maximum level of fluorescence was detected after 14 days of incubation (fig. 36).

ASCs treated with HA-based hydrogels showed the highest level of fluorescence after 7 days of incubation. After 14 days of HA incubation, the red fluorescence was generally less intense and almost undetectable using the Hyal-DUO hydrogel (fig. 37).

4.2.2.3.2. FID-119 sponge

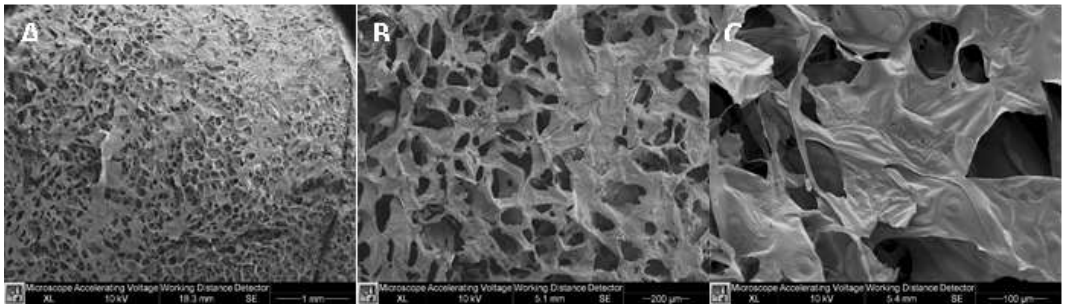


**Fig. 38.** FID-119 ultrastructural microscopy. SEM performed on samples of FID-119 evidenced a lamellar structure characterized by small alveoli and HA segments vertically oriented. FID-119 appeared as microporous material with smooth lamellar layers.

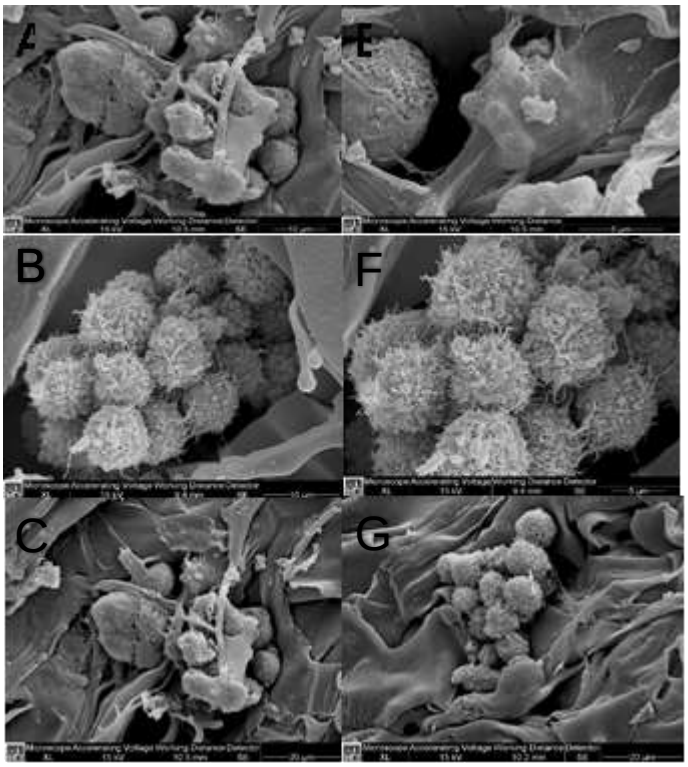


**Fig. 39.** SEM of FID-119 cultured with ASCs after 24 hours. The images clearly show the interaction between the ASCs and the hyaluronic acid fibers. ASCs are characterized by spherical shapes and rough membranes. Moreover, cells self-organize into clusters.

Fig. 38 shows the FID-119 ultrastructure obtained by SEM. The sponge appeared as a microporous material with small alveoli and smooth lamellar layers.

24 hours after incubation numerous alveoli were populated by cells, as shown in Fig. 39. At SEM, cells appeared characterized by spherical shape and rough membrane and they organized in clusters.

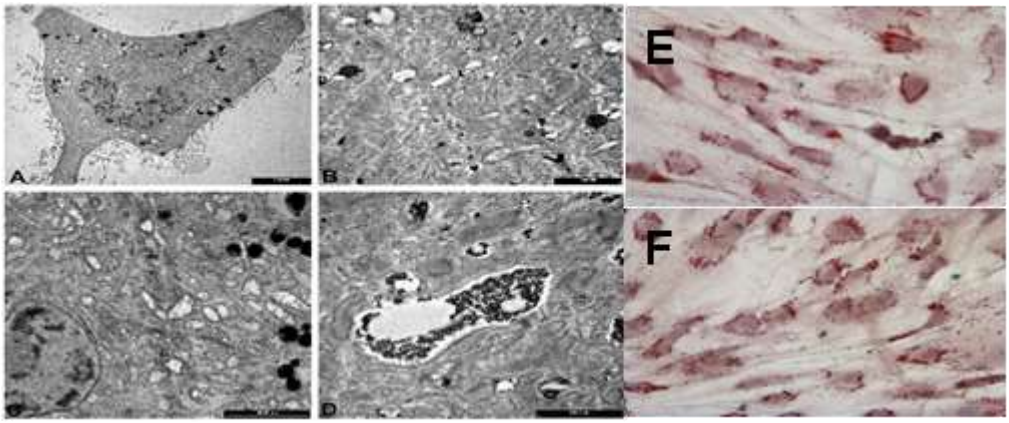


**Fig. 40.** TEM (A-D) and optical microscopy after staining with Red Oil O (E-F) after 24 hours. Few lipid droplets were visible.

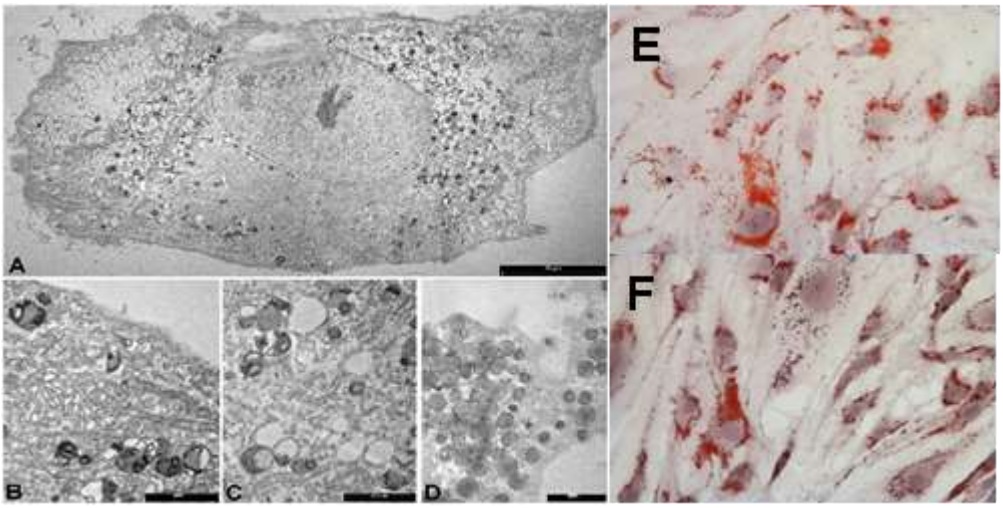


**Fig. 41.** TEM (A-D) and optical microscopy after staining with Oil Red O (E-F) after 7 days. The lipid change incremented and also Golgi apparatus and endoplasmic reticulum were abundant and well detectable.

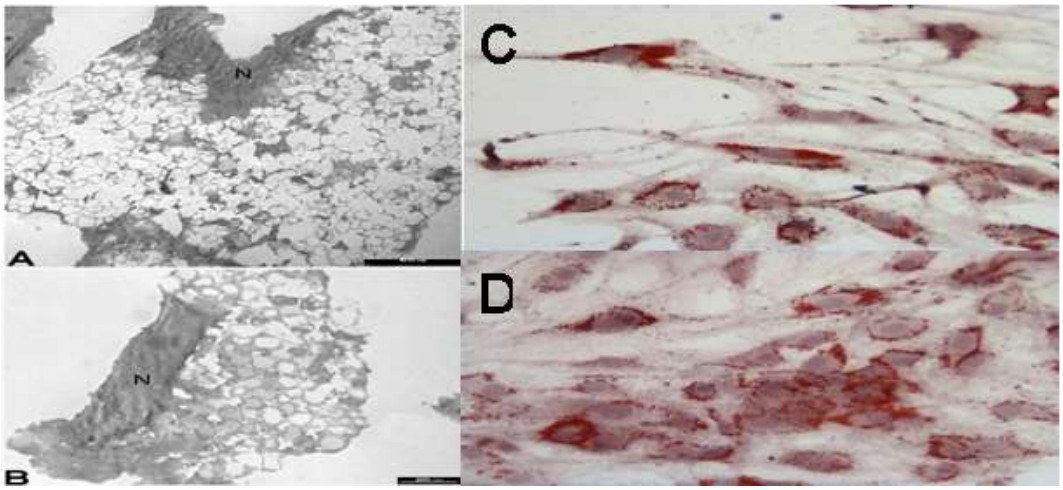


**Fig. 42.** TEM (A-B) and optical microscopy after staining with Oil Red O (C-D) after 14 days. TEM images clearly shows that the cytoplasm was completely full of lipid droplets and the nucleus was flat and near the cytoplasmic membrane. The cell morphology was typical of a mature adipocyte. Optical microscopy images confirm the abundance of lipid droplets.

After 24 hours from incubation with FID-119, at TEM, ADAS appeared characterized by irregular shape and by the presence of small lipid droplets in the cytosol (fig. 40. A). At higher magnifications numerous mitochondria and glycogen depots were detectable (fig. 40.B, 40.C, 40.D).

At optical microscope after staining with Oil Red O (fig. 40.E, 40.F) few lipid droplets were visible.

After 7 day from incubation with FID-119, Golgi apparatus and endoplasmic reticulum were more abundant and well-detectable at TEM (fig. 41.A, 41.B, 41.C, 41.D)

Observing Oil Red O stained cells through optical microscope, the lipid charge appeared incremented. (fig. 41.E, 41.F)

After 14 days from incubation with FID-119, the nucleus was located in a peripheral position (fig. 42.A, 42.B) and the cell cytoplasm was richer of lipid droplets (fig. 42.C, 42.D).

#### *4.2.2.4. Discussion*

In the present study, different hyaluronic acid formulations, specifically three powders and three fillers of different molecular weights were tested for their safety and their ability to promote ASCs adipogenic differentiation *in vitro*.

Since the resultant cell death rate of ASCs treated with all the hyaluronic acid powders and fillers was comparable with the negative control and much lower than the positive control, it was demonstrated that no formulation was cytotoxic.

Furthermore, since the expression of GLUT4 was high, the hyaluronic acid powders and fillers generally promoted the adipogenesis of ASCs *in vitro*.

Finally, ultrastructural and optical analysis showed that ASCs, once incubated with FID-119 hyaluronic acid sponge *in vitro*, interacted with and started to modify their morphology even after 24 hours, becoming mature adipocytes after 14 days.

#### *4.2.2.5. Conclusion*

The present study clearly evidences how different formulations of hyaluronic acid are safe and able to promote the adipogenic differentiation of ASCs. Biomolecular analysis will be performed in order to assess the level of expression of specific adipogenic markers.

### 4.2.3. *In vivo* interaction among hyaluronic acid and fat

#### *4.2.3.1. Introduction*

The present study aims to investigate the effect of combination of hyaluronic acid and fat grafting in tissue reconstruction and regeneration. Specifically, some *in vivo* experiments are presented and they had the following objectives:

1. to evaluate the volume maintenance over time of the FID-119 sponge combined with fat grafting compared to the sponge alone and fat grafting alone;

2. to evaluate the adipogenesis process, through histological analyses on the excised implants.

#### *4.2.3.2. Material and methods*

##### 4.2.3.2.1. Hyaluronic acid formulations

Hyaluronic acid FID-119 sponge (200 kDa), provided by Fidia Framaceutici SpA (Abano Terme, Padua, Italy) was tested in this *in vivo* study.

##### 4.2.3.2.2. Adipose tissue collection

Adipose tissue was harvested by 8 women subjected to liposuction, aging between 41 and 62 years old. Patients signed the informed consents before the tissue collection. The water-assisted liposuction named BEAULI® protocol was used. It is described in detail in [72].

##### 4.2.3.2.3. Animals

60 homozygote male nude mice, five weeks old, weighting 28-30 g, were purchased from Harlan Laboratories (Udine, Italy). They were housed in a temperature- and humidity- controlled environment, having free access to mouse chow and tap water, following the instruction of Interdepartmental Centre of Experimental Research Service (CIRSAL) of Verona University. Mice were randomly divided in three groups:

1. control group: 20 mice undergoing subcutaneous injection of adipose tissue (fat grafting);

2. control group: 20 mice undergoing subcutaneous implantation of the FID-119 sponge;

3. experimental group: 20 mice undergoing fat grafting together with the implantation of the FID-119 sponge.

For subcutaneous grafts, animals were anesthetized with a mixture of air and isofluorane 2%, positioned on heated bed in prone position, incised on the right flank and grafted with sponges and/or adipose tissue depending on the belonging group.

#### 4.2.3.2.4. Magnetic resonance imaging (MRI)

MRI was performed using a spectrometer operating at 4.7 T and equipped with an actively shielded gradient system (Bruker, Germany) having a maximum gradient strength of 40 G/cm. The animals were anesthetized by inhalation of a mixture of air and oxygen containing 0.5% of isofluorane, and placed in supine position in a 35 mm inner-diameter, birdcage coil. A sensor for breath monitoring was positioned at the level of the animal chest. The monitoring of subcutaneous implants was performed used axial and sagittal oriented T2-weighted sequences having the following parameters: TE= 56 ms; TR= 5000 ms; FOV= 4x4 cm2; slice thickness 0.1 cm=; flip angle = 180°, MTX= 256x256 pixels, NEX=1.

#### 4.2.3.2.5. 3D reconstruction of subcutaneous implants

The DICOM data acquired by MRI were imported into Amira 5.2.0. The segmentation was performed with semi-automatic software tools (mainly blow tool) and completed manually slice by slice. The display surface was rendered with high resolution and shading.

#### 4.2.3.2.6. Histology of subcutaneous implants

After 14 days from the implantation, mice were sacrificed and subcutaneous grafts were excised. Specimens were fixed in 10% buffered formalin for 2 hours, dehydrated by immersion in a graded ethanol series, clarified in xylene and paraffin embedded. Sections of 5 µm were obtained using a microtome equipped with rotating blade. Sections were stained with hematoxylin and eosin and then observed at light microscope Olympus BX-51, equipped with Nikon CCD camera and Image ProPlus 7.2 software.

#### *4.2.3.3. Results*

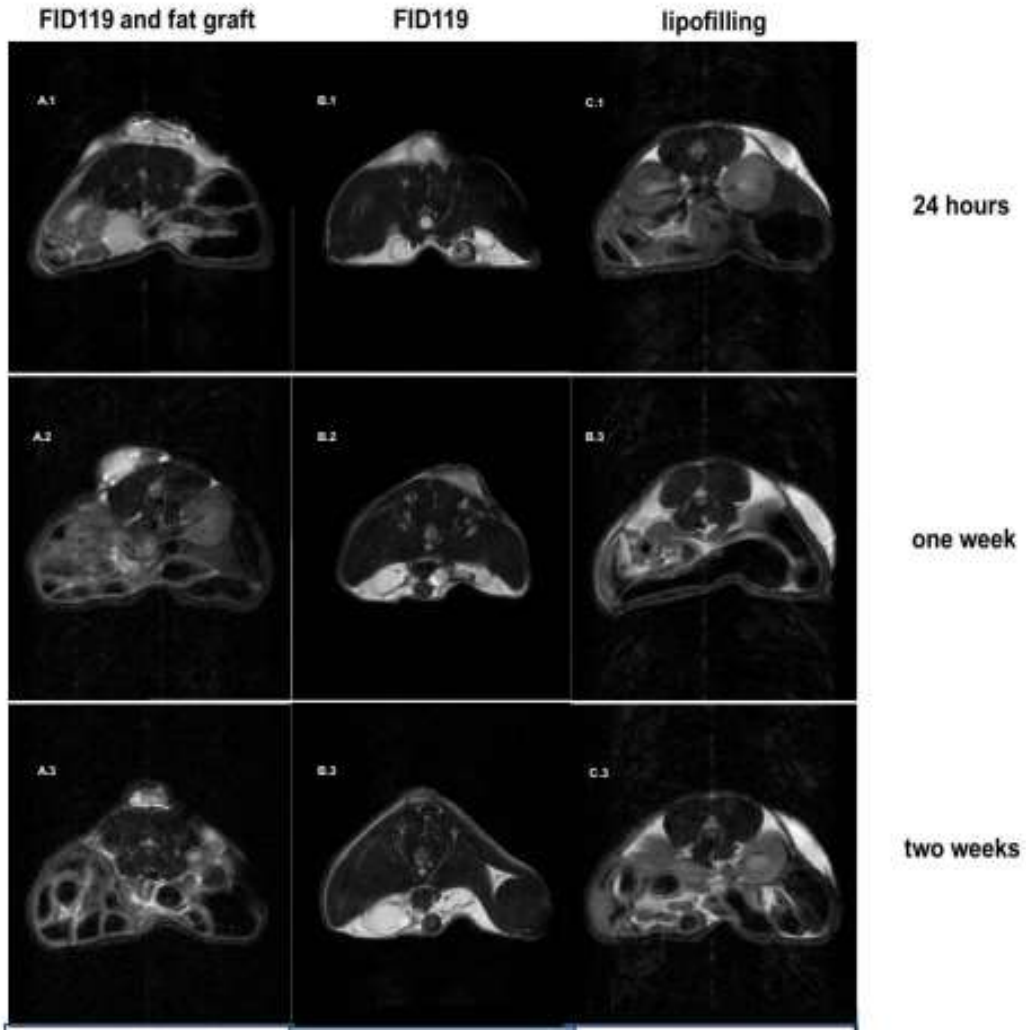


**Fig. 43.** MRI of implanted volumes after 24 hours (A.1-B.1-C.1), 1 week (A.2-B.2-C.2) and 2 weeks (A.3-B.3-C.3). The implant is represented by the sponge and adipose tissue (A.1-A.2-A.3), the sponge alone (B.1-B.2-B.3) and adipose tissue alone (C.1-C.2-C.3).

MRI show a good maintenance of volumes over time, when the implant is constituted by adipose tissue and FID-119 together (Fig. 43.A.1, 43.A.2, 43.A.3), and, to a lesser extent, adipose tissue alone (Fig. 43.C.1, 43.C.2, 43.C.3).

On the contrary, FID-119 alone was more rapidly adsorbed and almost not more visible after two weeks from the implantation (Fig. 43.B.1, 43.B.2, 43.B.3).

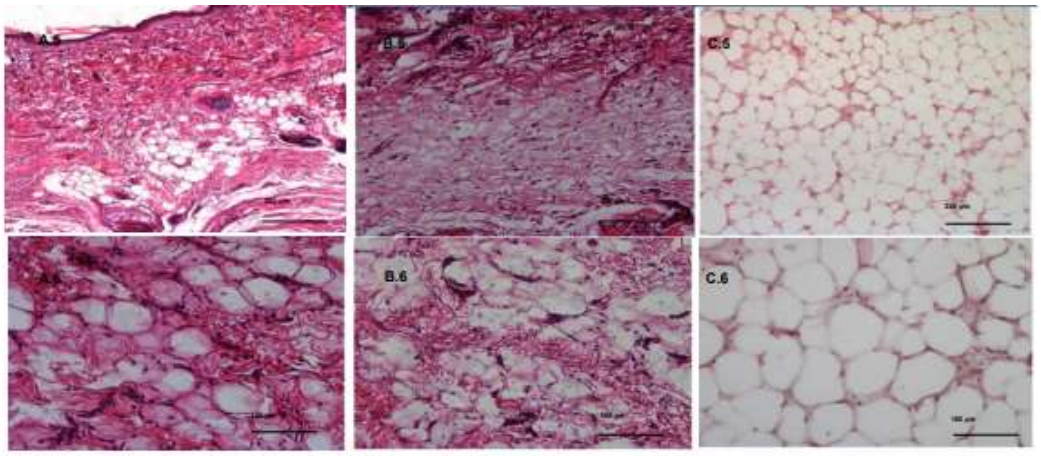


**Fig. 44.** Histological analysis. It was performed on sections of excised implants of sponge and adipose tissue (A.5-A.6), sponge alone (B.5-B.6) and adipose tissue alone (C.5-C.6).

The excised implants of adipose tissue and FID-119 show large portions of adipose tissue, probably of new formation, in the lamellar structure of HA-based scaffolds. Adipocytes were characterized by well-preserved membranes and circular shapes typical of mature adipocytes. A low-grade of inflammation was observable (fig. 44.A.5, 44.A.6).

The excised implants of FID-119 alone were characterized by lamellar aspect with some interposed adipocytes. Cells were characterized by unilocular aspect but had reduced dimensions of 40-50 µm. Moreover, adipocytes appeared stressed and their membranes were sometimes broken (fig. 44.B.5, 44.B.6).

The excised implants of adipose tissue alone were characterized by the typical aspect of adipose tissue. Adipocytes were unilocular, had thin membranes and circular shape. The dimension of adipocytes ranged between 50 and 70 µm (fig. 44.C.5, 44.C.6).

#### *4.2.3.4. Discussion*

In the present study, a hyaluronic acid sponge was tested for its ability to promote adipogenic differentiation *in vivo*, when implanted together with the injection of some adipose tissue. Specifically, MRI for testing the maintenance of volume over time and histology were performed, using the sponge alone and the fat grafting alone as controls.

The best results in terms of volume maintenance were obtained with the combination of sponge and fat. Also, the histology showed a good interaction between the sponge and the adipose tissue and the formation of new adipocytes.

#### *4.2.3.5. Conclusion*

The present study suggests that the hyaluronic acid sponge well interacts with fat grafting and is able to promote adipogenic differentiation. However, biomolecular analysis will be performed in order to assess the level of expression of specific adipogenic markers and confirm the qualitative data.

# *5. CONCLUSION*

Beside adipose tissue had been considered a discard product for many years, recently its role as regenerative agent has been widely recognized. It is especially played by its multipotent stromal cells, ASCs, cells characterized by self-renewal and multipotency properties.

This thesis has presented two different strategies to reconstruct or repair damaged tissues and organs through adipose tissue: autologous fat transfer and adipose tissue engineering. In the autologous fat transfer, autologous adipose tissue is harvested from one part of the body, purified through some processing techniques and reinjected where necessary. In tissue engineering, some scaffolds made of natural or synthetic materials, in this case hyaluronic acid, are used in combination with ASCs and, sometimes, growth factors to repair or reconstruct tissues. Both the strategies have been demonstrated to be effective at least *in vitro*, but further studies both *in vitro*, but especially *in vivo*, need to be performed.

The scientific community should intensify the study of adipose tissue, both in its theoretical and applied aspects, because this tissue surely hides other many interesting potentialities in reconstructive and regenerative surgery, but also in many other fields of medicine!

# *6. REFERENCES*


[1] V. M. Hsu, C. A. Stransky, L. P. Bucky, and I. Percec, "Fat grafting's past, present, and future: Why adipose tissue is emerging as a critical link to the advancement of regenerative medicine," *Aesthetic Surg. J.*, vol. 32, no. 7, pp. 892–899, 2012.

[2] E. E. Kershaw and J. S. Flier, "Adipose tissue as an endocrine organ," in *Journal of Clinical Endocrinology and Metabolism*, 2004, vol. 89, no. 6, pp. 2548–2556.

[3] M. Dashty, "Differential Role of AMP-Activated Protein Kinase in Brown and White Adipose Tissue Components and its Consequences in Metabolic Diseases," 2014.

[4] L. Szablewski, "Introductory Chapter: Types of Adipose Tissue," in *Adipose Tissue*, InTech, 2018.

[5] G. B. Bernasochi, J. R. Bell, E. R. Simpson, L. M. D. Delbridge, and W. C. Boon, "Impact of estrogens on the regulation of white, beige, and brown adipose tissue depots," *Compr. Physiol.*, vol. 9, no. 2, pp. 457–475, Apr. 2019.

[6] S. Cinti and R. Vettor, "The adipose organ," in *Adipose Tissue and Inflammation*, CRC Press, 2009, pp. 1–21.

[7] M. Hassan, N. Latif, and M. Yacoub, "Adipose tissue: friend or foe?," *Nat. Rev. Cardiol.*, vol. 9, no. 12, pp. 689–702, Dec. 2012.

[8] J. H. Choi *et al.*, "Adipose tissue engineering for soft tissue regeneration," *Tissue Engineering - Part B: Reviews*, vol. 16, no. 4. pp. 413–426, 01-Aug-2010.

[9] "How Beige Fat Could Fight Obesity | UC San Francisco." [Online]. Available: https://www.ucsf.edu/news/2015/04/124476/researchers-identify-calorie-burning-'beige'-fat-humans. [Accessed: 03-Nov-2019].

[10] M. M. Ibrahim, "Subcutaneous and visceral adipose tissue: structural and functional differences.," *Obes. Rev.*, vol. 11, no. 1, pp. 11–8, Jan. 2010.

[11] P. Bourin *et al.*, "Stromal cells from the adipose tissue-derived stromal vascular fraction and culture expanded adipose tissue-derived stromal/stem cells: A joint statement of the International Federation for Adipose Therapeutics and Science (IFATS) and the International Society for Cellular Therapy (ISCT)," *Cytotherapy*, vol. 15, no. 6, pp. 641–648, Jun. 2013.

[12] P. Bianco, "'Mesenchymal' Stem Cells," *Annu. Rev. Cell Dev. Biol.*, vol. 30, no. 1, pp. 677–704, 2014.

[13] P. Bianco, P. G. Robey, and P. J. Simmons, "Mesenchymal Stem Cells: Revisiting History, Concepts, and Assays," *Cell Stem Cell*, vol. 2, no. 4, pp. 313–319, 2008.

[14] M. Dominici *et al.*, "Minimal criteria for defining multipotent mesenchymal stromal cells. The International Society for Cellular Therapy position statement.," *Cytotherapy*, vol. 8, no. 4, pp. 315–7, 2006.

[15] Y. Jiang *et al.*, "Pluripotency of mesenchymal stem cells derived from adult marrow," vol. 418, no. July, 2002.

[16] M. F. Pittenger *et al.*, "Multilineage Potential of Adult Human Mesenchymal Stem Cells," *Science (80-. ).*, vol. 284, no. April, pp. 143–147, 1999.

[17] D. G. Phinney and D. J. Prockop, "Concise review: mesenchymal stem/multipotent stromal cells: the state of transdifferentiation and modes of tissue repair--current views.," *Stem Cells*, vol. 25, no. 11, pp. 2896–2902, 2007.

[18] B. Sacchetti *et al.*, “Self-Renewing Osteoprogenitors in Bone Marrow Sinusoids Can Organize a Hematopoietic Microenvironment,” *Cell*, vol. 131, no. 2, pp. 324–336, 2007.

[19] J. R. Ferreira, G. Q. Teixeira, S. G. Santos, M. A. Barbosa, G. Almeida-Porada, and R. M. Gonçalves, “Mesenchymal Stromal Cell Secretome: Influencing Therapeutic Potential by Cellular Pre-conditioning,” *Frontiers in immunology*, vol. 9. NLM (Medline), p. 2837, 2018.

[20] G. Rigotti *et al.*, “Clinical Treatment of Radiotherapy Tissue Damage by Lipoaspirate Transplant: A Healing Process Mediated by Adipose-Derived Adult Stem Cells,” *Plast. Reconstr. Surg.*, vol. 119, no. 5, pp. 1409–1422, 2007.

[21] P. A. Zuk *et al.*, “Human adipose tissue is a source of multipotent stem cells.,” *Mol. Biol. Cell*, vol. 13, no. 12, pp. 4279–95, Dec. 2002.

[22] D. Peroni *et al.*, “Stem molecular signature of adipose-derived stromal cells,” *Exp. Cell Res.*, vol. 314, no. 3, pp. 603–615, 2008.

[23] M. Al-Nbaheen *et al.*, “Human Stromal (Mesenchymal) Stem Cells from Bone Marrow, Adipose Tissue and Skin Exhibit Differences in Molecular Phenotype and Differentiation Potential,” *Stem Cell Rev. Reports*, vol. 9, no. 1, pp. 32–43, 2013.

[24] G. Constantin *et al.*, “Adipose-derived mesenchymal stem cells ameliorate chronic experimental autoimmune encephalomyelitis,” *Stem Cells*, vol. 27, no. 10, pp. 2624–2635, 2009.

[25] R. Dai, Z. Wang, R. Samanipour, K. Koo, and K. Kim, “Adipose-derived stem cells for tissue engineering and regenerative medicine applications,” *Stem Cells Int.*, vol. 2016, 2016.

[26] S. Wakao *et al.*, “Multilineage-differentiating stress-enduring (Muse) cells are a primary source of induced pluripotent stem cells in human fibroblasts.,” *Proc. Natl. Acad. Sci. U. S. A.*, vol. 108, no. 24, pp. 9875–

9880, 2011.

[27] S. Wakao, Y. Kuroda, F. Ogura, T. Shigemoto, and M. Dezawa, "Regenerative Effects of Mesenchymal Stem Cells: Contribution of Muse Cells, a Novel Pluripotent Stem Cell Type that Resides in Mesenchymal Cells," *Cells*, vol. 1, no. 4, pp. 1045–1060, 2012.

[28] F. Ogura *et al.*, "Human adipose tissue possesses a unique population of pluripotent stem cells with nontumorigenic and low telomerase activities: potential implications in regenerative medicine.," *Stem Cells Dev.*, vol. 23, no. 7, pp. 717–28, 2014.

[29] E. Bellini, M. P. Grieco, and E. Raposio, "The science behind autologous fat grafting," *Annals of Medicine and Surgery*, vol. 24. Elsevier Ltd, pp. 65–73, 01-Dec-2017.

[30] F. Simonacci, N. Bertozzi, M. P. Grieco, E. Grignaffini, and E. Raposio, "Procedure, applications, and outcomes of autologous fat grafting," *Annals of Medicine and Surgery*, vol. 20. Elsevier Ltd, pp. 49–60, 01-Aug-2017.

[31] S. R. Coleman, "Structural fat grafts: the ideal filler?," *Clin. Plast. Surg.*, vol. 28, no. 1, pp. 111–9, Jan. 2001.

[32] S. R. Coleman, "Structural fat grafting: more than a permanent filler.," *Plast. Reconstr. Surg.*, vol. 118, no. 3 Suppl, pp. 108S-120S, Sep. 2006.

[33] A. Monfort and A. Izeta, "Strategies for Human Adipose Tissue Repair and Regeneration," *J. Cosmet. Dermatological Sci. Appl.*, vol. 2, pp. 93–107, 2012.

[34] F. Simonacci, N. Bertozzi, M. P. Grieco, and E. Raposio, "From liposuction to adipose-derived stem cells: Indications and technique," *Acta Biomed.*, vol. 90, no. 2, pp. 197–208, 2019.

[35] "FAT GRAFTING (FAT INJECTION) (FAT TRANSFER)." [Online]. Available: https://www.sweng.sg/fat-grafting-fat-injection-fat-transfer/. [Accessed: 03-Nov-2019].

[36] M. Doornaert, J. Colle, E. De Maere, H. Declercq, and P. Blondeel, "Autologous fat grafting: Latest insights," *Annals of Medicine and Surgery*, vol. 37. Elsevier Ltd, pp. 47–53, 01-Jan-2019.

[37] J. Laloze *et al.*, "Cell-assisted lipotransfer: Friend or foe in fat grafting? Systematic review and meta-analysis," *Journal of Tissue Engineering and Regenerative Medicine*, vol. 12, no. 2. John Wiley and Sons Ltd, pp. e1237–e1250, 01-Feb-2018.

[38] T. Fontes, I. Brandão, R. Negrão, M. J. Martins, and R. Monteiro, "Autologous fat grafting: Harvesting techniques," *Annals of Medicine and Surgery*, vol. 36. Elsevier Ltd, pp. 212–218, 01-Dec-2018.

[39] M. J. Landau, Z. E. Birnbaum, L. G. Kurtz, and J. A. Aronowitz, "Review: Proposed methods to improve the survival of adipose tissue in autologous fat grafting," *Plast. Reconstr. Surg. - Glob. Open*, vol. 6, no. 8, pp. 1–7, 2018.

[40] V. Cervelli *et al.*, "Application of platelet-rich plasma in plastic surgery: Clinical and in vitro evaluation," *Tissue Eng. - Part C Methods*, vol. 15, no. 4, pp. 625–634, Dec. 2009.

[41] V. Cervelli, L. Palla, M. Pascali, B. De Angelis, B. C. Curcio, and P. Gentile, "Autologous platelet-rich plasma mixed with purified fat graft in aesthetic plastic surgery," *Aesthetic Plast. Surg.*, vol. 33, no. 5, pp. 716–721, Sep. 2009.

[42] J. Choi, K. W. Minn, and H. Chang, "The efficacy and safety of platelet-rich plasma and adipose-derived stem cells: An update," *Arch. Plast. Surg.*, vol. 39, no. 6, pp. 585–592, Nov. 2012.

[43] Y. C. Por, V. K. L. Yeow, N. Louri, T. K. H. Lim, I. Kee, and I. C. Song, "Platelet-rich plasma has no effect on increasing free fat graft survival in the nude mouse," *J. Plast. Reconstr. Aesthetic Surg.*, vol. 62, no. 8, pp. 1030–1034, Aug. 2009.

[44] J. M. Serra-Renom, J. M. Serra-Mestre, J. M. Serra-Renom, and J. M. Serra-Mestre, “Fat Grafting: Principles and General Concepts,” in *Atlas of Minimally Invasive Facelift*, Springer International Publishing, 2016, pp. 11–16.

[45] E. D. Buckingham, “Fat transfer techniques: general concepts.,” *Facial Plast. Surg.*, vol. 31, no. 1, pp. 22–8, Feb. 2015.

[46] A. Trivisonno *et al.*, “Concise Review: Intraoperative Strategies for Minimal Manipulation of Autologous Adipose Tissue for Cell- and Tissue-Based Therapies,” *Stem Cells Transl. Med.*, p. sctm.19-0166, 2019.

[47] E. Raposio and R. G. Ciliberti, “Clinical use of adipose-derived stem cells: European legislative issues,” *Ann. Med. Surg.*, vol. 24, pp. 61–64, Dec. 2017.

[48] F. De Francesco, S. Mannucci, G. Conti, E. Dai Prè, A. Sbarbati, and M. Riccio, “A Non-Enzymatic Method to Obtain a Fat Tissue Derivative Highly Enriched in Adipose Stem Cells (ASCs) from Human Lipoaspirates: Preliminary Results.,” *Int. J. Mol. Sci.*, vol. 19, no. 7, 2018.

[49] F. Bianchi *et al.*, “A new nonenzymatic method and device to obtain a fat tissue derivative highly enriched in pericyte-like elements by mild mechanical forces from human lipoaspirates.,” *Cell Transplant.*, vol. 22, no. 11, pp. 2063–77, 2013.

[50] A. Casadei *et al.*, “Adipose tissue regeneration: A state of the art,” *Journal of Biomedicine and Biotechnology*, vol. 2012. 2012.

[51] M. Pfaff, W. Wu, E. Zellner, and D. M. Steinbacher, “Processing technique for lipofilling influences adipose-derived stem cell concentration and cell viability in lipoaspirate,” *Aesthetic Plast. Surg.*, vol. 38, no. 1, pp. 224–229, 2014.

[52] E. C. Cleveland, N. J. Albano, and A. Hazen, “Roll, Spin, Wash, or Filter? Processing of Lipoaspirate for Autologous Fat Grafting: An Updated,

Evidence-Based Review of the Literature.," *Plast. Reconstr. Surg.*, vol. 136, no. 4, pp. 706–13, 2015.

[53] A. L. Strong, P. S. Cederna, J. P. Rubin, S. R. Coleman, and B. Levi, "The Current State of Fat Grafting: A Review of Harvesting, Processing, and Injection Techniques.," *Plast. Reconstr. Surg.*, vol. 136, no. 4, pp. 897–912, 2015.

[54] A. Conde-Green *et al.*, "Comparison of 3 Techniques of Fat Grafting and Cell-Supplemented Lipotransfer in Athymic Rats: A Pilot Study," *Aesthetic Surg. J.*, vol. 33, no. 5, pp. 713–721, 2013.

[55] J. G. Rose *et al.*, "Histologic comparison of autologous fat processing methods.," *Ophthal. Plast. Reconstr. Surg.*, vol. 22, no. 3, pp. 195–200, 2006.

[56] A. Condé-Green *et al.*, "Effects of centrifugation on cell composition and viability of aspirated adipose tissue processed for transplantation.," *Aesthet. Surg. J.*, vol. 30, no. 2, pp. 249–255, 2010.

[57] A. Cond??-Green, N. F. Gontijo De Amorim, and I. Pitanguy, "Influence of decantation, washing and centrifugation on adipocyte and mesenchymal stem cell content of aspirated adipose tissue: A comparative study," *J. Plast. Reconstr. Aesthetic Surg.*, vol. 63, no. 8, pp. 1375–1381, 2010.

[58] H. M. Salinas *et al.*, "Comparative Analysis of Processing Methods in Fat Grafting.," *Plast. Reconstr. Surg.*, pp. 675–683, 2014.

[59] A. Gabriel, M. C. Champaneria, and G. P. Maxwell, "Fat grafting and breast reconstruction: tips for ensuring predictability.," *Gland Surg.*, vol. 4, no. 3, pp. 232–23243, 2015.

[60] P. Gir, S. A. Brown, G. Oni, N. Kashefi, A. Mojallal, and R. J. Rohrich, "Fat grafting: Evidence-based review on autologous fat harvesting, processing, reinjection, and storage," *Plastic and Reconstructive Surgery*, vol. 130, no. 1. pp. 249–258, Jul-2012.

[61] E. Oberbauer, C. Steffenhagen, C. Wurzer, C. Gabriel, H. Redl, and S. Wolbank, “Enzymatic and non-enzymatic isolation systems for adipose tissue-derived cells: current state of the art.,” *Cell Regen. (London, England)*, vol. 4, p. 7, 2015.

[62] H. Pinto and J. Fontdevila, Eds., *Regenerative Medicine Procedures for Aesthetic Physicians*. Cham: Springer International Publishing, 2019.

[63] P. Gentile, M. G. Scioli, A. Bielli, A. Orlandi, and V. Cervelli, “Comparing different nanofat procedures on scars: Role of the stromal vascular fraction and its clinical implications,” *Regen. Med.*, vol. 12, no. 8, pp. 939–952, Dec. 2017.

[64] F. Svolacchia, F. De Francesco, L. Trovato, A. Graziano, and G. A. Ferraro, “An innovative regenerative treatment of scars with dermal micrografts,” *J. Cosmet. Dermatol.*, vol. 15, no. 3, pp. 245–253, Sep. 2016.

[65] R. Miranda, E. Farina, and M. A. Farina, “Micrografting chronic lower extremity ulcers with mechanically disaggregated skin using a micrograft preparation system,” *J. Wound Care*, vol. 27, no. 2, pp. 60–65, Feb. 2018.

[66] F. De Francesco *et al.*, “A Regenerative Approach with Dermal Micrografts in the Treatment of Chronic Ulcers,” *Stem Cell Rev. Reports*, vol. 13, no. 1, pp. 139–148, Feb. 2017.

[67] P. Gentile *et al.*, “Platelet-Rich Plasma and Micrografts Enriched with Autologous Human Follicle Mesenchymal Stem Cells Improve Hair Re-Growth in Androgenetic Alopecia. Biomolecular Pathway Analysis and Clinical Evaluation,” *Biomedicines*, vol. 7, no. 2, p. 27, Apr. 2019.

[68] M. Viganò *et al.*, “Rationale and pre-clinical evidences for the use of autologous cartilage micrografts in cartilage repair,” *J. Orthop. Surg. Res.*, vol. 13, no. 1, p. 279, Dec. 2018.

[69] M. Monti *et al.*, “In Vitro and In Vivo Differentiation of Progenitor Stem Cells Obtained After Mechanical Digestion of Human Dental Pulp,” *J.*

*Cell. Physiol.*, vol. 232, no. 3, pp. 548–555, Mar. 2017.

[70] S. Kawakami, M. Shiota, K. Kon, M. Shimogishi, and S. Kasugai, "The Effect of Dissociated Soft Tissue on Osteogenesis: A Preliminary In Vitro Study," *Int. J. Oral Maxillofac. Implants*, vol. 34, no. 3, pp. 651–657, May 2019.

[71] F. Zanzottera, E. Lavezzari, L. Trovato, A. Icardi, and A. Graziano, "Adipose Derived Stem Cells and Growth Factors Applied on Hair Transplantation. Follow-Up of Clinical Outcome," *J. Cosmet. Dermatological Sci. Appl.*, vol. 4, pp. 268–274, 2014.

[72] K. Ueberreiter, U. Tanzella, F. Cromme, D. Doll, and B. D. Krapohl, "One stage rescue procedure after capsular contracture of breast implants with autologous fat grafts collected by water assisted liposuction ('BEAULI Method').," *GMS Interdiscip. Plast. Reconstr. Surg. DGPW*, vol. 2, p. Doc03, 2013.

[73] "(1) HY TISSUE SVF Instructions for use - YouTube." [Online]. Available: https://www.youtube.com/watch?v=m_o9FFHHHKI. [Accessed: 10-Nov-2019].

[74] P. Tonnard, A. Verpaele, G. Peeters, M. Hamdi, M. Cornelissen, and H. Declercq, "Nanofat grafting: Basic research and clinical applications," *Plast. Reconstr. Surg.*, vol. 132, no. 4, pp. 1017–1026, 2013.

[75] "(1) Description of a new closed system to process fat and to obtain nanofat: Analysis of clinical and cytometric results." [Online]. Available: https://www.researchgate.net/publication/317443427_Description_of_a_new_closed_system_to_process_fat_and_to_obtain_nanofat_Analysis_of_clinical_and_cytometric_results. [Accessed: 01-Dec-2019].

[76] A. Shafiee and A. Atala, "Tissue Engineering: Toward a New Era of Medicine," *Annu. Rev. Med.*, vol. 68, no. 1, pp. 29–40, Jan. 2017.

[77] M. N. Collins and C. Birkinshaw, "Hyaluronic acid based scaffolds for

tissue engineering - A review," *Carbohydrate Polymers*, vol. 92, no. 2. pp. 1262–1279, 15-Feb-2013.

[78] B. Bakhshandeh *et al.*, "Tissue engineering; strategies, tissues, and biomaterials.," *Biotechnol. Genet. Eng. Rev.*, vol. 33, no. 2, pp. 144–172, Oct. 2017.

[79] R. N. Babita Mahanta, "An Overview of Various Biomimetic Scaffolds: Challenges and Applications in Tissue Engineering," *J. Tissue Sci. Eng.*, vol. 05, no. 02, 2014.

[80] C. E. Schanté, G. Zuber, C. Herlin, and T. F. Vandamme, "Chemical modifications of hyaluronic acid for the synthesis of derivatives for a broad range of biomedical applications," *Carbohydrate Polymers*, vol. 85, no. 3. pp. 469–489, 01-Jun-2011.

[81] N. M. Salwowska, K. A. Bebenek, D. A. Żądło, and D. L. Wcisło-Dziadecka, "Physiochemical properties and application of hyaluronic acid: a systematic review.," *J. Cosmet. Dermatol.*, vol. 15, no. 4, pp. 520–526, Dec. 2016.

[82] M. Hemshekhar, R. M. Thushara, S. Chandranayaka, L. S. Sherman, K. Kemparaju, and K. S. Girish, "Emerging roles of hyaluronic acid bioscaffolds in tissue engineering and regenerative medicine," *Int. J. Biol. Macromol.*, vol. 86, pp. 917–928, 2016.

[83] E. Dai Prè, G. Conti, and A. Sbarbati, "Hyaluronic Acid (HA) Scaffolds and Multipotent Stromal Cells (MSCs) in Regenerative Medicine," *Stem Cell Rev. Reports*, vol. 12, no. 6, pp. 664–681, 2016.